

VIBRATION CHARACTERISTICS OF ELLIPTIC AND ELLIPSOIDAL THIN SHELL

A Thesis Submitted to the
Graduate School of Natural and Applied Sciences of
Dokuz Eylül University

In Partial Fullfillment of the Requirements for
the Degree Master of Science in Mechanical Engineering,
Machine Theory and Dynamics Program

138845

by

Aydın Doğu YILDIRIM

September, 2003

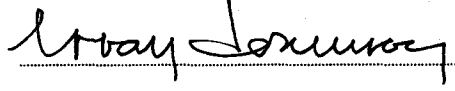
İZMİR

138845

T.C. YÖKSEKÖĞRETİM KURULU
DOKÜMANTASYON MERKEZİ

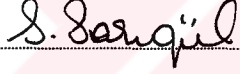
M.Sc THESIS EXAMINATION RESULT FORM

We certify that we have read this thesis and “**VIBRATION CHARACTERISTICS OF ELLIPTIC AND ELLIPSOIDAL THIN SHELL**” completed by **AYDIN DOĞU YILDIRIM** under supervision of **Prof. Dr. ERKAN DOKUMACI** and that in our opinion it is fully adequate, in scope and in quality, as a thesis for the degree of Master of Science.



Prof. Dr. E. DOKUMACI

Supervisor



Doç. Dr. SAHİDE SARIĞÜL

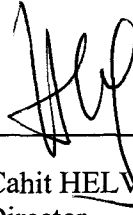
(Committee Member)



Yrd. Doç. Dr. BİLENTİ YARDIMCI

(Committee Member)

Approved by the
Graduate School of Natural and Applied Sciences




Prof. Dr. Cahit HELVACI
Director

ACKNOWLEDGEMENTS

I would like to express my gratitude to Prof. Dr. Erkan DOKUMACI for his guidance throughout this study.

I am also very indebted to my father İzzet YILDIRIM and my mother Nevin YILDIRIM for their encouragement, patience and endless support.



Aydın Dođu YILDIRIM

ABSTRACT

In this thesis study; vibration characteristics of elliptical and circular cylindrical, spheroidal (ellipsoid of revolution) and ellipsoidal thin shells are investigated. The main goal of the study is to find the first few resonance frequencies of the thin shells which have these types of geometries. This aim is achieved by finding the natural frequencies of the shells.

The geometrical and physical equations of the investigated shells have been derived by using the differential geometry mathematics and “Love thin shell theory”. A finite element method with ring elements has been developed by using the energy expressions, for obtaining the numerical results. These results have been obtained by computer programmes which have been written in MATLAB.

The results found by; the vibration experiment, the commercial analysis software IDEAS and the thesis study, have been compared to prove the validity of the derived equations and the written MATLAB programmes. A satisfactory harmony has been observed during the comparisons.

Keywords: Vibration, thin shells, resonance, finite element method, elliptic and ellipsoidal geometries.

ÖZET

Bu tez çalışmasında; eliptik ve dairesel silindirik, sferoidal (dönel elipsoid) ve elipsoidal ince kabukların titreşim karakteristikleri incelenmektedir. Çalışmanın esas amacı, bu geometrilere sahip ince kabukların ilk birkaç rezonans frekanslarını bulmaktır. Bu amaca, kabukların doğal frekanslarının bulunmasıyla ulaşılmaktadır.

İncelenen kabukların geometrik ve fiziksel denklemleri, diferansiyel geometri matematiği ve “Love ince kabuk teorisi” kullanılarak çıkarılmıştır. Nümerik sonuçların elde edilmesi için enerji denklemleri kullanılarak halka elemanlı sonlu elemanlar metodu geliştirilmiştir. Bu sonuçlar, MATLAB’de yazılmış olan bilgisayar programları ile elde edilmiştir.

Çıkarılan denklemlerin ve yazılmış olan MATLAB programlarının doğruluğunu ispat etmek için; titreşim deneyi sonuçları, ticari bir analiz programı olan IDEAS ile elde edilen sonuçlar ve tez çalışması ile bulunan sonuçlar karşılaştırılmıştır. Yapılan karşılaştırmalar sırasında tatmin edici bir uyum gözlemlenmiştir.

Anahtar sözcükler: Titreşim, ince kabuklar, rezonans, sonlu elemanlar metodu, eliptik ve elipsoidal geometriler.

CONTENTS

	Page
Contents	IV
List of Tables	VII
List of Figures	VIII
Nomenclature	X

Chapter One

INTRODUCTION

1.1 Introduction	1
------------------------	---

Chapter Two

THEORETICAL CONSIDERATIONS

2.1 Representation of Shell Geometry in Curvilinear Coordinates	5
2.1.1 Shell Coordinates and Fundamental Forms	5
2.1.2 Fundamental Forms and Their Coefficients	6
2.1.3 Lamé' Parameters and Radii of Principle Curvatures	9
2.2 Geometric Properties of Cylinders and Ellipsoids	10
2.2.1 Geometric Properties of Cylinders	10
2.2.2 Geometric Properties of Ellipsoids	14

2.3 Shell Equations	18
2.3.1 General Strain-Displacement Relations with Love Simplifications....	18
2.3.2 Strain-Displacement Relations for Cylindrical Thin Shells	20
2.3.3 Strain-Displacement Relations for Ellipsoidal (also Spheroidal) Thin Shells	21

Chapter Three

SOLUTION PROCEDURE

3.1 Strain and Kinetic Energy Expressions for Thin Shells	23
3.1.1 Strain Energy	23
3.1.2 Kinetic Energy	26
3.2 Ring Elements for Cylindrical and Spheroidal Shells	27
3.2.1 Ring Element Technique Used for Finite Element Modeling	27
3.3 Approximate Ring Elements for Elliptic and Ellipsoidal Shells	34

Chapter Four

NUMERICAL RESULTS AND COMPARATIVE EXAMPLES

4.1 Results for Some Cylindrical and Spheroidal Thin Shell Structures	36
4.2 Results for Some Elliptical and Ellipsoidal Thin Shell Structures	41

Chapter Five

EXPERIMENT RESULTS

5.1 Experimental Setup and Procedure	42
--	----

Chapter Six
CONCLUSIONS

6.1 Conclusions	47
REFERENCES	49
APPENDICES	51
APPENDIX 1: MatLab Codes of “Free.m” Programme	51



LIST OF TABLES

	Page
Table 4.1 Comparison of natural frequencies obtained by different solution sources for Fig.4.1. (circumferential mode number, $n_2=3$)	37
Table 4.2 Comparison of natural frequencies obtained by different solution sources for Fig.4.2. (circumferential mode number, $n_1=1$)	38
Table 4.3 Comparison of natural frequencies obtained by different solution sources for Fig.4.3. (circumferential mode number, $n_1=1$)	39
Table 4.4 Comparison of natural frequencies obtained by different solution sources for Fig. 4.4. (circumferential mode numbers of spheroid cap and cylinder, $n_1=1, n_2=1$)	40
Table 4.5 Fundamental natural frequencies for elliptical and ellipsoidal shells obtained by finite element programmes	41
Table 5.1 Numerical presentation of Fig. 5.3	46

LIST OF FIGURES

	Page
Figure 2.1 Arbitrary shell geometry and location of a point on it	6
Figure 2.2 Unit normal vector	6
Figure 2.3 Elliptical cylinder in curvilinear coordinates	10
Figure 2.4 Circular cylinder in curvilinear coordinates	13
Figure 2.5 Ellipsoidal shell in curvilinear coordinates	14
Figure 2.6 Spheroidal shell in curvilinear coordinates	17
Figure 3.1 One ring finite element for circular cylinder	29
Figure 3.2 One ring finite element for spheroid	30
Figure 3.3 The whole finite element model for circular cylinder	32
Figure 3.4 The whole finite element model for spheroid	33
Figure 4.1 The simple supported cylinder at both edges that lets axial motion (File1.m). ($a=b=60$ mm, cylinder length $L=120$ mm, $h=3$ mm, $\mu=0.3$, $E=206$ GPa, $\rho=7860$ kg/m ³)	37
Figure 4.2 The spheroidal thin shell clamped at cut edge (File2.m). ($a=b=45$ mm, $c=85$ mm, length $Z=65$ mm, $h=3.5$ mm, $\mu=0.3$, $E=206$ GPa, $\rho=7860$ kg/m ³)	38
Figure 4.3 The spheroidal thin shell clamped at cut edge (File3.m). ($a=b=80$ mm, $c=60$ mm, length $Z=35$ mm, $h=3.5$ mm, $\mu=0.3$, $E=206$ GPa, $\rho=7860$ kg/m ³)	39
Figure 4.4 The thin shell formed by the combination of a half spheroidal and a circular cylindrical thin shell which is clamped at cylindrical edge (File4.m). ($a=b=75$ mm, $c=30$ mm, cylinder length $L=60$ mm, $h=3.5$ mm, $\mu=0.3$, $E=206$ GPa, $\rho=7860$ kg/m ³)	40

- Figure 5.1 Schematic illustration of the test equipment connection 42
- Figure 5.2 Thin shell structure wanted to be tested for fully free boundary condition.
($c=30$ mm, $L=60$ mm, $h=3.5$ mm, $\mu=0.3$, $E=206$ GPa, $\rho=7860$ kg/m³,
 $a=b=75$ mm for Model – I; $a=77$ mm, $b=73$ mm for Model – II) 44
- Figure 5.3 Comparison of numerical (Model-I & Model-II) and experimental results
(circumferential mode numbers of numerical results for cap and cylinder
are respectively (2,1), (3,1), (4,1), (5,1), (6,1), (7,1), (8,1)) 46



NOMENCLATURE

A_1, A_2	Fundamental form parameters (Lame' parameters)
a, b, c	Geometric parameters
b_{11}, b_{12}, b_{22}	Coefficients of second fundamental form
D	Bending stiffness
E	Elasticity modulus
f_{11}, f_{12}, f_{22}	Coefficients of third fundamental form
g_{11}, g_{12}, g_{22}	Coefficients of first fundamental form
G	Shear modulus
h	Shell thickness
\mathbf{I}	Unit matrix
k	Bending strain
\mathbf{k}	Stiffness matrix
K	Membrane stiffness
L	Lagrangian
\mathbf{m}	Mass matrix
\mathbf{N}	Unit normal vector
n	Circumferential mode number
P	Potential (strain) energy
R	Dissipation function
R_1, R_2	Radii of principle curvatures
s_k, s_{k+1}	General α_2 measures for any ring element
T	Kinetic energy
u_1, u_2, u_3	Displacements in the direction of curvilinear coordinates

U	Displacement function
U_1, U_2, U_3	Polynomial functions
\mathbf{U}	Displacement matrix
$\dot{\mathbf{U}}$	Velocity matrix
V	Volume
w	Natural frequency
x, y, z	Cartesian coordinates
Z, L	Length parameters
I, II, III	First, second and third fundamental forms
$\alpha_1, \alpha_2, \alpha_3$	Curvilinear coordinates
β_1, β_2	Angles in displacement formulation
ε	Strain
ε^o	Membrane strain
φ	Phase angle
κ_1, κ_2	Principle curvatures
μ	Poisson's ratio
ρ	Mass density
σ_{ij}	Stress term

CHAPTER ONE

INTRODUCTION

1.1 INTRODUCTION

This thesis is concerned with the vibration characteristics of cylindrical, spheroidal and ellipsoidal thin shells. The main goal of the study is to determine the primary resonance frequencies.

Vibration can often lead to a number of undesirable circumstances. For example, vibration of an automobile or truck can lead to driver discomfort and eventually, fatigue. Structural or mechanical failure can often result from sustained vibration. Because of these reasons, governments, international agencies and also manufacturers set desired vibration performance standards for some products. To avoid from these vibration problems care should be taken in the design stage. In design, the natural frequencies of a structure or machine are extremely important in predicting and understanding a system's dynamic behavior. The primary requirement of widely performed vibration tests is a determination of a system's natural frequencies. And if the measured frequencies agree with those predicted by the analytical model, the model is verified and can be used in design with some confidence.

The fundamental idea behind the study is the resonance phenomena. Because of the rapid rise in vibration magnitudes, probability of the structure fatigue and noise problems, resonance comes out one of the major vibration problems. The natural frequencies of shell structures must be known in order to avoid the destructive effect of resonance with nearby rotating or reciprocating machinery. As the driving

frequency approaches the natural frequency of a lightly damped structure, resonance occurs. This means that the vibration of the structure is in a harmony with the driving force frequency; hence the excitation strongly supports the vibration magnitude. For lightly damped structures the resonance frequencies may be taken to be equal to its undamped natural frequencies. In general, the knowledge of the first few natural frequencies gives an opportunity to avoid coincidence with the driving (forcing) frequency.

The vibration of thin shells has received the attention of many authors. There is an extensive literature on the subject, and many shell theories have been proposed (Soedel, 1993), (Donnell, 1976), (Markus, 1988).

The foundations of the 'classical' theory of thin shells were established by Love, who was the first to formulate the preconditions for thin shells. Love's preconditions are also termed *Love's approximation of the first kind*, (Markus, 1988) and they were originally published in 1892. These are: (1) the shell is thin; (2) the deflections are small; (3) normal stresses perpendicular to the middle surface can be neglected in comparison to the other stresses; (4) normals to the reference surface remain normal to it during deflection and undergo no change in length during deformation (Soedel, 1976). These preconditions are the background of any linear theory of thin shells. All subsequent theories aim at refining the original approximations introduced by Love.

The simplification which can be made by use of the Love's approximation is very great, as it permits the displacement of every point in the shell wall, and hence the strains and stresses at every point, to be defined in terms of the displacement of one surface such as the middle surface of the shell wall. This represents in effect the reduction of the problem from three- to a two – dimensional one. The errors due to the Love approximations are negligible for 'thin shells' of homogeneous material. And it provides sufficiently accurate values for very much less computational effort in comparison with a three dimensional theory which is accurate but much more cumbersome. That is why the theory used in this thesis is "Love's thin shell theory".

For cylindrical (circular and elliptical), ellipsoidal and spheroidal thin shells, Lamé' Parameters and radius of curvatures have been found. And also the strain – displacement relations (with Love simplifications) have been derived for these geometries.

After giving the kinetic and strain energy expressions for thin shell structures, the ring element technique has been developed in F.E.M, for circular cylindrical and spheroidal shells. This ring element has an axisymmetric geometric shape which is used for shells of revolution. By using the ring finite element technique, the fundamental natural frequencies of some axisymmetric thin shell structures in different boundary conditions have been calculated. And the validity of these results is proved by analyzing the same structures with a well – known 'commercial' software IDEAS.

For elliptical and ellipsoidal thin shells, the validity of the same ring elements has been examined. Although the correct energy expressions have been used, the investigation shows that the displacement functions (sine or cosine) used for axisymmetric geometries do not give the completely true solution for elliptical and ellipsoidal shells. Because those ring elements have an asymmetric shape through the z-axis. This fact was observed during the experiment which has been performed for the half piece of a compressor shell. As this structure has an elliptical – like cross section, the results found by ring element model are not very close to the test results, but not very far from them; because the elliptic curvature effect is not very noticeable at the test structure. The experimental study has been performed to check the reliability of the theoretical derivations and ring element formulation procedure. It has been seen that the experimental study supports the theoretical calculations. The performed experimental study is based on the frequency spectrum analysis of an impulse excitation. By this experimental procedure the first few resonance frequencies could be found.

The present thesis consists of five chapters. Presented in Chapter 2 are an analysis of general shell geometry, and the strain – displacement relations that are required

for formulating the energy expressions, in a generality encompassing elliptical and ellipsoidal thin shells.

Chapter 3 presents the strain and kinetic energy expressions for thin shells and a finite element formulation is given. Ring elements are the fundamental implements of the procedure.

“Numerical Results and Comparative Examples” is the title of Chapter 4. In this chapter numerical results are given for some shell geometries and boundary conditions. And these results are compared with the I-DEAS (cad/cam software) results for the same shell types.

Experiment procedure and experimental measurement of a shell structure and the numerical results related to that shell are presented in Chapter 5. The numerical calculations and the physical results of the experiment are compared.

CHAPTER TWO

THEORETICAL CONSIDERATIONS

In this chapter, geometric equations and principal shell equations are presented. These equations form the basis of the solution procedure.

2.1 REPRESENTATION OF SHELL GEOMETRY IN CURVILINEAR COORDINATES

2.1.1 Shell Coordinates and Fundamental Forms

It is assumed that thin, isotropic and homogenous shells of constant thickness have neutral surfaces (Soedel, 1993). Locations on the neutral surface, placed into a three-dimensional Cartesian coordinate system, can also be defined by two – dimensional curvilinear surface coordinates α_1 and α_2 , as shown by equation (2.2). Because of this, curvilinear and Cartesian coordinates are related and the location of a point P on the neutral surface (see Fig.2.1) can be expressed as $P(x_1, x_2, x_3)$ or $P(\alpha_1, \alpha_2)$.

$$x_1 = f_1(\alpha_1, \alpha_2), \quad x_2 = f_2(\alpha_1, \alpha_2), \quad x_3 = f_3(\alpha_1, \alpha_2). \quad (2.1)$$

The location of P can also be expressed by a vector \mathbf{r} .

$$\mathbf{r}(\alpha_1, \alpha_2) = f_1(\alpha_1, \alpha_2)\mathbf{e}_1 + f_2(\alpha_1, \alpha_2)\mathbf{e}_2 + f_3(\alpha_1, \alpha_2)\mathbf{e}_3, \quad (2.2)$$

where \mathbf{e}_i is the unit vector, $i = 1, 2, 3$.

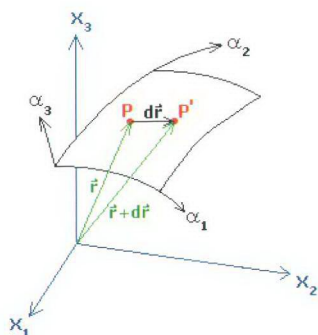


Figure 2.1 Arbitrary shell geometry and location of a point on it.

2.1.2 Fundamental Forms and Their Coefficients

Vector \mathbf{N} (see Fig.2.2) should be defined to obtain all of the fundamental forms. It is the unit normal vector of the neutral surface and is given by (Akbulut, 1970)

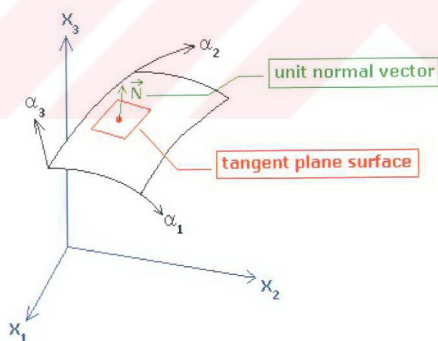


Figure 2.2 Unit normal vector.

$$\mathbf{N} = \frac{\frac{\partial \mathbf{r}}{\partial \alpha_1} \times \frac{\partial \mathbf{r}}{\partial \alpha_2}}{\left| \frac{\partial \mathbf{r}}{\partial \alpha_1} \times \frac{\partial \mathbf{r}}{\partial \alpha_2} \right|} = \frac{\frac{\partial \mathbf{r}}{\partial \alpha_1} \times \frac{\partial \mathbf{r}}{\partial \alpha_2}}{\sqrt{\left(\frac{\partial \mathbf{r}}{\partial \alpha_1} \times \frac{\partial \mathbf{r}}{\partial \alpha_2} \right) \cdot \left(\frac{\partial \mathbf{r}}{\partial \alpha_1} \times \frac{\partial \mathbf{r}}{\partial \alpha_2} \right)}}. \quad (2.3)$$

The differential changes $d\mathbf{r}$ and $d\mathbf{N}$ are

$$d\mathbf{r} = \frac{\partial \mathbf{r}}{\partial \alpha_1} d\alpha_1 + \frac{\partial \mathbf{r}}{\partial \alpha_2} d\alpha_2, \quad d\mathbf{N} = \frac{\partial \mathbf{N}}{\partial \alpha_1} d\alpha_1 + \frac{\partial \mathbf{N}}{\partial \alpha_2} d\alpha_2. \quad (2.4)$$

Essentially, there are three fundamental forms and these can be shown practically and generally by a matrix as given by (Akbulut, 1970)

$$\begin{pmatrix} I & II & III \\ d\mathbf{N} & d\mathbf{r} & 0 \\ 0 & d\mathbf{N} & d\mathbf{r} \end{pmatrix}. \quad (2.5)$$

Here, I , II and III are respectively *first*, *second* and *third fundamental forms*:

$$I = \begin{vmatrix} d\mathbf{r} & 0 \\ d\mathbf{N} & d\mathbf{r} \end{vmatrix} = d\mathbf{r} \cdot d\mathbf{r} = \left(\frac{\partial \mathbf{r}}{\partial \alpha_1} d\alpha_1 + \frac{\partial \mathbf{r}}{\partial \alpha_2} d\alpha_2 \right) \cdot \left(\frac{\partial \mathbf{r}}{\partial \alpha_1} d\alpha_1 + \frac{\partial \mathbf{r}}{\partial \alpha_2} d\alpha_2 \right), \quad (2.6)$$

$$II = - \begin{vmatrix} d\mathbf{N} & 0 \\ 0 & d\mathbf{r} \end{vmatrix} = -d\mathbf{N} \cdot d\mathbf{r} = - \left(\frac{\partial \mathbf{N}}{\partial \alpha_1} d\alpha_1 + \frac{\partial \mathbf{N}}{\partial \alpha_2} d\alpha_2 \right) \cdot \left(\frac{\partial \mathbf{r}}{\partial \alpha_1} d\alpha_1 + \frac{\partial \mathbf{r}}{\partial \alpha_2} d\alpha_2 \right), \quad (2.7)$$

$$III = \begin{vmatrix} d\mathbf{N} & d\mathbf{r} \\ 0 & d\mathbf{N} \end{vmatrix} = d\mathbf{N} \cdot d\mathbf{N} = \left(\frac{\partial \mathbf{N}}{\partial \alpha_1} d\alpha_1 + \frac{\partial \mathbf{N}}{\partial \alpha_2} d\alpha_2 \right) \cdot \left(\frac{\partial \mathbf{N}}{\partial \alpha_1} d\alpha_1 + \frac{\partial \mathbf{N}}{\partial \alpha_2} d\alpha_2 \right), \quad (2.8)$$

$$I = g_{11}(d\alpha_1)^2 + 2g_{12}d\alpha_1d\alpha_2 + g_{22}(d\alpha_2)^2, \quad (2.9)$$

$$II = b_{11}(d\alpha_1)^2 + 2b_{12}d\alpha_1d\alpha_2 + b_{22}(d\alpha_2)^2, \quad (2.10)$$

$$III = f_{11}(d\alpha_1)^2 + 2f_{12}d\alpha_1d\alpha_2 + f_{22}(d\alpha_2)^2, \quad (2.11)$$

where the coefficients are

$$g_{11} = \frac{\partial \mathbf{r}}{\partial \alpha_1} \cdot \frac{\partial \mathbf{r}}{\partial \alpha_1}, \quad (2.12a)$$

$$g_{12} = 0 \quad (\text{for orthogonal coordinates}), \quad (2.12b)$$

$$g_{22} = \frac{\partial \mathbf{r}}{\partial \alpha_2} \cdot \frac{\partial \mathbf{r}}{\partial \alpha_2}, \quad (2.12c)$$

$$b_{11} = -\frac{\partial \mathbf{N}}{\partial \alpha_1} \cdot \frac{\partial \mathbf{r}}{\partial \alpha_1}, \quad b_{11} = \frac{\partial^2 \mathbf{r}}{\partial \alpha_1^2} \cdot \mathbf{N}, \quad (2.13a)$$

$$b_{12} = -\frac{1}{2} \left(\frac{\partial \mathbf{N}}{\partial \alpha_1} \cdot \frac{\partial \mathbf{r}}{\partial \alpha_2} + \frac{\partial \mathbf{N}}{\partial \alpha_2} \cdot \frac{\partial \mathbf{r}}{\partial \alpha_1} \right), \quad \text{or as given by} \quad b_{12} = \frac{\partial^2 \mathbf{r}}{\partial \alpha_1 \partial \alpha_2} \cdot \mathbf{N}, \quad (2.13b)$$

$$b_{22} = -\frac{\partial \mathbf{N}}{\partial \alpha_2} \cdot \frac{\partial \mathbf{r}}{\partial \alpha_2}, \quad b_{22} = \frac{\partial^2 \mathbf{r}}{\partial \alpha_2^2} \cdot \mathbf{N}, \quad (2.13c)$$

$$f_{11} = \frac{\partial \mathbf{N}}{\partial \alpha_1} \cdot \frac{\partial \mathbf{N}}{\partial \alpha_1}, \quad (2.14a)$$

$$f_{12} = 0 \quad (\text{for orthogonal coordinates}), \quad (2.14b)$$

$$f_{22} = \frac{\partial \mathbf{N}}{\partial \alpha_2} \cdot \frac{\partial \mathbf{N}}{\partial \alpha_2}. \quad (2.14c)$$

2.1.3 Lamé Parameters and Radii of Principle Curvatures

Here, Lamé Parameters and radii of the principle curvatures are stated. These terms will be used in physical shell equations and in some calculations. They are (Kreyszig, 1959):

$$A_1 = \sqrt{g_{11}}, \quad (2.15)$$

$$A_2 = \sqrt{g_{22}}, \quad (2.16)$$

which are called *Lamé Parameters* or *Fundamental Form Parameters*. Beside this,

$$\kappa_1 = \frac{b_{11}}{g_{11}} \quad \text{and} \quad \kappa_2 = \frac{b_{22}}{g_{22}}, \quad (2.17)$$

are the principle curvatures of the shell, and

$$R_1 = \frac{1}{|\kappa_1|}, \quad (2.18)$$

$$R_2 = \frac{1}{|\kappa_2|}, \quad (2.19)$$

are the radii of principle curvatures.

2.2 GEOMETRIC PROPERTIES OF CYLINDERS AND ELLIPSOIDS

2.2.1 Geometric Properties of Cylinders

It is the aim of the study to present the geometric properties of a cylindrical shell. Generally, an elliptical cylindrical shell looks like as shown in Fig. 2.3.

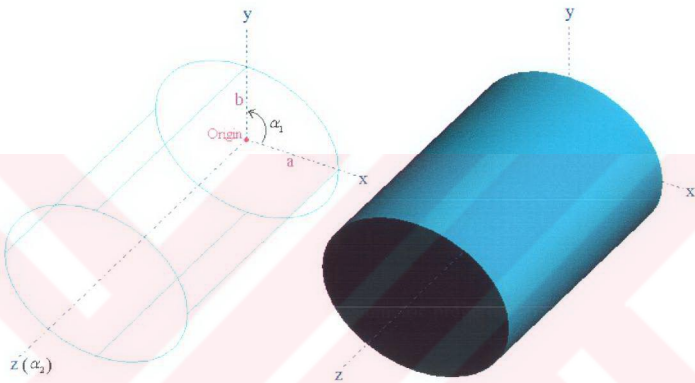


Figure 2.3 Elliptical cylinder in curvilinear coordinates.

A point on the surface of the shell can be defined by using the orthogonal curvilinear coordinates, as given by (Lipschutz, 1969)

$$\mathbf{r} = a \cos \alpha_1 \mathbf{e}_1 + b \sin \alpha_1 \mathbf{e}_2 + \alpha_2 \mathbf{e}_3, \quad (2.20)$$

where $0 \leq \alpha_1 \leq 2\pi$.

Here, α_1 is the curvilinear coordinate about the center of the ellipse and on the xy -plane. And α_2 is the longitudinally variable through the z -axis.

The differential properties of an elliptical cylindrical shell become

$$\frac{\partial \mathbf{r}}{\partial \alpha_1} = -a \sin \alpha_1 \mathbf{e}_1 + b \cos \alpha_1 \mathbf{e}_2 + 0 \mathbf{e}_3, \quad (2.21)$$

$$\frac{\partial^2 \mathbf{r}}{\partial \alpha_1^2} = -a \cos \alpha_1 \mathbf{e}_1 - b \sin \alpha_1 \mathbf{e}_2 + 0 \mathbf{e}_3, \quad (2.22)$$

$$\frac{\partial^2 \mathbf{r}}{\partial \alpha_1 \partial \alpha_2} = 0 \mathbf{e}_1 + 0 \mathbf{e}_2 + 0 \mathbf{e}_3, \quad (2.23)$$

$$\frac{\partial \mathbf{r}}{\partial \alpha_2} = 0 \mathbf{e}_1 + 0 \mathbf{e}_2 + 1 \mathbf{e}_3, \quad (2.24)$$

$$\frac{\partial^2 \mathbf{r}}{\partial \alpha_2^2} = 0 \mathbf{e}_1 + 0 \mathbf{e}_2 + 0 \mathbf{e}_3. \quad (2.25)$$

By substituting these into the equations in section 2.1, it can be found that

$$\mathbf{N} = \frac{\frac{\partial \mathbf{r}}{\partial \alpha_1} \times \frac{\partial \mathbf{r}}{\partial \alpha_2}}{\left| \frac{\partial \mathbf{r}}{\partial \alpha_1} \times \frac{\partial \mathbf{r}}{\partial \alpha_2} \right|} = \frac{b \cos \alpha_1 \mathbf{e}_1 + a \sin \alpha_1 \mathbf{e}_2 + 0 \mathbf{e}_3}{\sqrt{(b \cos \alpha_1)^2 + (a \sin \alpha_1)^2}}, \quad (2.26)$$

$$g_{11} = (a \sin \alpha_1)^2 + (b \cos \alpha_1)^2, \quad (2.27a)$$

$$g_{12} = 0, \quad (2.27b)$$

$$g_{22} = 1, \quad (2.27c)$$

$$h_{11} = \frac{-ab(\cos^2 \alpha_1 + \sin^2 \alpha_1)}{\sqrt{(b \cos \alpha_1)^2 + (a \sin \alpha_1)^2}} = \frac{-ab}{\sqrt{(b \cos \alpha_1)^2 + (a \sin \alpha_1)^2}}, \quad (2.28a)$$

$$b_{12} = 0, \quad (2.28b)$$

$$b_{22} = 0. \quad (2.28c)$$

The Lamé' parameters, A_1 and A_2 are

$$A_1 = \sqrt{(a \sin \alpha_1)^2 + (b \cos \alpha_1)^2}, \quad (2.29)$$

$$A_2 = 1, \quad (2.30)$$

$$\kappa_1 = \frac{b_{11}}{g_{11}} = \frac{-ab}{\sqrt{(b \cos \alpha_1)^2 + (a \sin \alpha_1)^2}} = \frac{-ab}{[(b \cos \alpha_1)^2 + (a \sin \alpha_1)^2]^{(3/2)}}, \quad (2.31)$$

$$\kappa_2 = \frac{b_{22}}{g_{22}} = \frac{0}{1} = 0. \quad (2.32)$$

The radii of the curvatures, R_1 and R_2 are

$$R_1 = \frac{1}{|\kappa_1|} = \frac{[(b \cos \alpha_1)^2 + (a \sin \alpha_1)^2]^{(3/2)}}{ab}, \quad (2.33)$$

$$R_2 = \frac{1}{|\kappa_2|} = \infty. \quad (2.34)$$

If parameter b is equalized to parameter a , then the elliptical cylinder turns to be a circular cylinder and it is illustrated in Fig. (2.4).

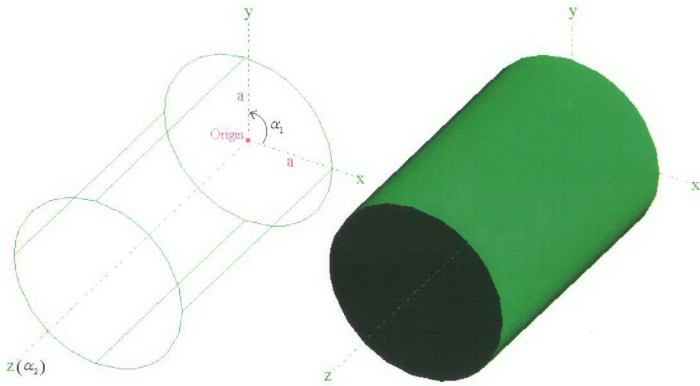


Figure 2.4 Circular cylinder in curvilinear coordinates.

By substituting $b=a$ in equations (2.29), (2.30), (2.33) and (2.34), the Lamé parameters and radii of curvatures of a circular cylinder can be easily found. These are given at the below.

$$A_1 = \sqrt{(a \sin \alpha_1)^2 + (a \cos \alpha_1)^2} = a, \quad (2.35)$$

$$A_2 = 1, \quad (2.36)$$

$$R_1 = \frac{[(a \cos \alpha_1)^2 + (a \sin \alpha_1)^2]^{(3/2)}}{a^2} = a, \quad (2.37)$$

$$R_2 = \infty. \quad (2.38)$$

2.2.2 Geometric Properties of Ellipsoids

The general equation for ellipsoids is (Thomas & Finney, 1992), referring to Fig. 2.5 for notation,

$$\frac{x^2}{a^2} + \frac{y^2}{b^2} + \frac{z^2}{c^2} = 1. \quad (2.39)$$

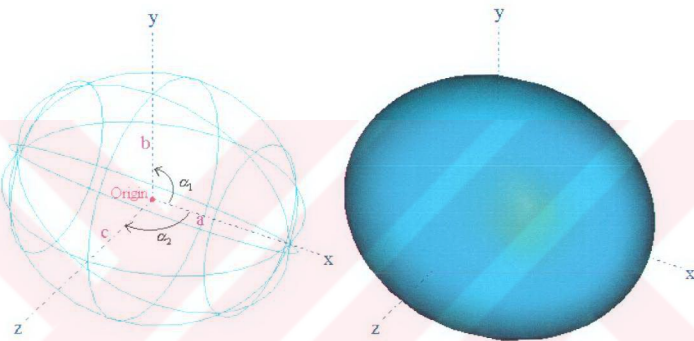


Figure 2.5 Ellipsoidal shell in curvilinear coordinates.

An arbitrary point on the surface of the shell can be defined by using the orthogonal curvilinear coordinates, as given by (Kreyszig, 1993)

$$\mathbf{r} = a \cos \alpha_2 \cos \alpha_1 \mathbf{e}_1 + b \cos \alpha_2 \sin \alpha_1 \mathbf{e}_2 + c \sin \alpha_2 \mathbf{e}_3, \quad (2.40)$$

where $0 \leq \alpha_1 \leq 2\pi$ and $-\pi/2 \leq \alpha_2 \leq \pi/2$.

Here, α_1 and α_2 are the curvilinear variables about the center of the ellipses in the xy - plane and the xz - plane respectively. So, the differential geometric properties of an ellipsoidal shell become

$$\frac{\partial \mathbf{r}}{\partial \alpha_1} = -a \cos \alpha_2 \sin \alpha_1 \mathbf{e}_1 + b \cos \alpha_2 \cos \alpha_1 \mathbf{e}_2 + 0 \mathbf{e}_3, \quad (2.41)$$

$$\frac{\partial^2 \mathbf{r}}{\partial \alpha_1^2} = -a \cos \alpha_2 \cos \alpha_1 \mathbf{e}_1 - b \cos \alpha_2 \sin \alpha_1 \mathbf{e}_2 + 0 \mathbf{e}_3, \quad (2.42)$$

$$\frac{\partial^2 \mathbf{r}}{\partial \alpha_1 \partial \alpha_2} = a \sin \alpha_2 \sin \alpha_1 \mathbf{e}_1 - b \sin \alpha_2 \cos \alpha_1 \mathbf{e}_2 + 0 \mathbf{e}_3, \quad (2.43)$$

$$\frac{\partial \mathbf{r}}{\partial \alpha_2} = -a \sin \alpha_2 \cos \alpha_1 \mathbf{e}_1 - b \sin \alpha_2 \sin \alpha_1 \mathbf{e}_2 + c \cos \alpha_2 \mathbf{e}_3, \quad (2.44)$$

$$\frac{\partial^2 \mathbf{r}}{\partial \alpha_2^2} = -a \cos \alpha_2 \cos \alpha_1 \mathbf{e}_1 - b \cos \alpha_2 \sin \alpha_1 \mathbf{e}_2 - c \sin \alpha_2 \mathbf{e}_3. \quad (2.45)$$

By substituting these into the equations in section 2.1, it can be found that

$$\mathbf{N} = \frac{\frac{\partial \mathbf{r}}{\partial \alpha_1} \times \frac{\partial \mathbf{r}}{\partial \alpha_2}}{\left| \frac{\partial \mathbf{r}}{\partial \alpha_1} \times \frac{\partial \mathbf{r}}{\partial \alpha_2} \right|} = \frac{cb \cos \alpha_2 \cos \alpha_1 \mathbf{e}_1 + ca \cos \alpha_2 \sin \alpha_1 \mathbf{e}_2 + ab \sin \alpha_2 \mathbf{e}_3}{\sqrt{(cb \cos \alpha_2 \cos \alpha_1)^2 + (ca \cos \alpha_2 \sin \alpha_1)^2 + (ab \sin \alpha_2)^2}}, \quad (2.46)$$

$$g_{11} = \cos^2 \alpha_2 \left[(a \sin \alpha_1)^2 + (b \cos \alpha_1)^2 \right], \quad (2.47a)$$

$$g_{12} = 0, \quad (2.47b)$$

$$g_{22} = (a \sin \alpha_2 \cos \alpha_1)^2 + (b \sin \alpha_2 \sin \alpha_1)^2 + (c \cos \alpha_2)^2, \quad (2.47c)$$

$$b_{11} = \frac{-cba \cos^2 \alpha_2}{\sqrt{(cb \cos \alpha_2 \cos \alpha_1)^2 + (ca \cos \alpha_2 \sin \alpha_1)^2 + (ab \sin \alpha_2)^2}}, \quad (2.48a)$$

$$b_{12} = \frac{cba(\sin \alpha_2 \sin \alpha_1 \cos \alpha_2 \cos \alpha_1 - \sin \alpha_2 \sin \alpha_1 \cos \alpha_2 \cos \alpha_1)}{\sqrt{(cb \cos \alpha_2 \cos \alpha_1)^2 + (ca \cos \alpha_2 \sin \alpha_1)^2 + (ab \sin \alpha_2)^2}} = 0, \quad (2.48b)$$

$$b_{22} = \frac{-cba}{\sqrt{(cb \cos \alpha_2 \cos \alpha_1)^2 + (ca \cos \alpha_2 \sin \alpha_1)^2 + (ab \sin \alpha_2)^2}}. \quad (2.48c)$$

The Lamé' parameters, A_1 and A_2 are

$$A_1 = \cos \alpha_2 \sqrt{[(a \sin \alpha_1)^2 + (b \cos \alpha_1)^2]}, \quad (2.49)$$

$$A_2 = \sqrt{(a \sin \alpha_2 \cos \alpha_1)^2 + (b \sin \alpha_2 \sin \alpha_1)^2 + (c \cos \alpha_2)^2}, \quad (2.50)$$

$$\kappa_1 = \frac{b_{11}}{g_{11}} = \frac{-cba}{\sqrt{(cb \cos \alpha_2 \cos \alpha_1)^2 + (ca \cos \alpha_2 \sin \alpha_1)^2 + (ab \sin \alpha_2)^2} [(a \sin \alpha_1)^2 + (b \cos \alpha_1)^2]}, \quad (2.51)$$

$$\kappa_2 = \frac{b_{22}}{g_{22}} = \frac{-cba}{\sqrt{(cb \cos \alpha_2 \cos \alpha_1)^2 + (ca \cos \alpha_2 \sin \alpha_1)^2 + (ab \sin \alpha_2)^2} [(a \sin \alpha_2 \cos \alpha_1)^2 + (b \sin \alpha_2 \sin \alpha_1)^2 + (c \cos \alpha_2)^2]}. \quad (2.52)$$

The radii of the curvatures, R_1 and R_2 are

$$R_1 = \frac{1}{|\kappa_1|} = \frac{[(a \sin \alpha_1)^2 + (b \cos \alpha_1)^2] \sqrt{(cb \cos \alpha_2 \cos \alpha_1)^2 + (ca \cos \alpha_2 \sin \alpha_1)^2 + (ab \sin \alpha_2)^2}}{cba}, \quad (2.53)$$

$$R_2 = \frac{1}{|\kappa_2|} = \frac{[(a \sin \alpha_2 \cos \alpha_1)^2 + (b \sin \alpha_2 \sin \alpha_1)^2 + (c \cos \alpha_2)^2] \sqrt{(cb \cos \alpha_2 \cos \alpha_1)^2 + (ca \cos \alpha_2 \sin \alpha_1)^2 + (ab \sin \alpha_2)^2}}{cba}. \quad (2.54)$$

As it is known, an ellipsoid has three geometric parameters which are a , b and c . If two of these are equal to each other, then this type of ellipsoid is known as *ellipsoid of revolution* or *spheroid*. So, if parameter b is equalized to parameter a , then an ellipsoid turns to be a spheroid and it is illustrated in Fig. (2.6).

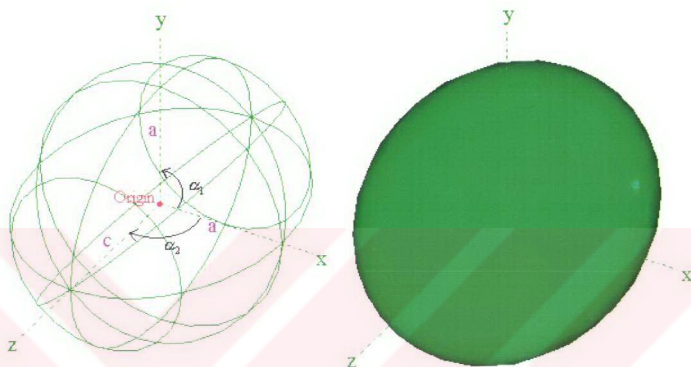


Figure 2.6 Spheroidal shell in curvilinear coordinates.

By substituting $b=a$ in equations (2.49), (2.50), (2.53) and (2.54), the Lamé' parameters and radii of curvatures of a spheroid can be easily found. These are given at the below.

$$A_1 = \cos \alpha_2 \sqrt{[(a \sin \alpha_1)^2 + (a \cos \alpha_1)^2]} = \cos(\alpha_2) a, \quad (2.55)$$

$$A_2 = \sqrt{(a \sin \alpha_2 \cos \alpha_1)^2 + (a \sin \alpha_2 \sin \alpha_1)^2 + (c \cos \alpha_2)^2}, \quad (2.56)$$

$$R_1 = \frac{\sqrt{(ca \cos \alpha_2 \cos \alpha_1)^2 + (ca \cos \alpha_2 \sin \alpha_1)^2 + (a^2 \sin \alpha_2)^2}}{c}, \quad (2.57)$$

$$R_2 = \frac{[(a \sin \alpha_2 \cos \alpha_1)^2 + (a \sin \alpha_2 \sin \alpha_1)^2 + (c \cos \alpha_2)^2] \sqrt{(ca \cos \alpha_2 \cos \alpha_1)^2 + (ca \cos \alpha_2 \sin \alpha_1)^2 + (a^2 \sin \alpha_2)^2}}{ca^2}. \quad (2.58)$$

2.3 SHELL EQUATIONS

Shell equations are based on the assumptions that the shells are thin with respect to their radii of curvature and deflections are reasonably small.

2.3.1 General Strain-Displacement Relations with Love Simplifications

Love (Soedel, 1993) proposed, that if a shell is thin, it may be assumed that the displacements in the α_1 and α_2 directions vary linearly through the shell thickness, whereas displacements in the α_3 direction are independent of α_3 ; that is,

$$U_1(\alpha_1, \alpha_2, \alpha_3) = u_1(\alpha_1, \alpha_2) + \alpha_3 \beta_1(\alpha_1, \alpha_2), \quad (2.59)$$

$$U_2(\alpha_1, \alpha_2, \alpha_3) = u_2(\alpha_1, \alpha_2) + \alpha_3 \beta_2(\alpha_1, \alpha_2), \quad (2.60)$$

$$U_3(\alpha_1, \alpha_2, \alpha_3) = u_3(\alpha_1, \alpha_2), \quad (2.61)$$

where β_1 and β_2 represent angles.

By this assumption, strains can be separated into membrane and bending types. Beside this, ε_{33} (normal strain) and ε_{13} , ε_{23} (shear strains) are neglected. And finally, strain – displacement relationships simplify to (Soedel, 1993)

$$\varepsilon_{33} = 0, \quad (2.62)$$

$$\varepsilon_{13} = 0, \quad (2.63)$$

$$\varepsilon_{23} = 0, \quad (2.64)$$

$$\varepsilon_{11} = \varepsilon_{11}^o + \alpha_3 k_{11}, \quad (2.65)$$

$$\varepsilon_{22} = \varepsilon_{22}^o + \alpha_3 k_{22}, \quad (2.66)$$

$$\varepsilon_{12} = \varepsilon_{12}^o + \alpha_3 k_{12}. \quad (2.67)$$

Here, ε_{11}^o , ε_{22}^o , ε_{12}^o are called the “membrane strains” (independent of α_3) and k_{11} , k_{22} , k_{12} are called the “bending strains” (proportional to α_3). These can be expressed as follows (Soedel, 1993):

$$\varepsilon_{11}^o = \frac{1}{A_1} \frac{\partial u_1}{\partial \alpha_1} + \frac{u_2}{A_1 A_2} \frac{\partial A_1}{\partial \alpha_2} + \frac{u_3}{R_1}, \quad (2.68)$$

$$\varepsilon_{22}^o = \frac{1}{A_2} \frac{\partial u_2}{\partial \alpha_2} + \frac{u_1}{A_1 A_2} \frac{\partial A_2}{\partial \alpha_1} + \frac{u_3}{R_2}, \quad (2.69)$$

$$\varepsilon_{12}^o = \frac{A_2}{A_1} \frac{\partial}{\partial \alpha_1} \left(\frac{u_2}{A_2} \right) + \frac{A_1}{A_2} \frac{\partial}{\partial \alpha_2} \left(\frac{u_1}{A_1} \right), \quad (2.70)$$

$$k_{11} = \frac{1}{A_1} \frac{\partial \beta_1}{\partial \alpha_1} + \frac{\beta_2}{A_1 A_2} \frac{\partial A_1}{\partial \alpha_2}, \quad (2.71)$$

$$k_{22} = \frac{1}{A_2} \frac{\partial \beta_2}{\partial \alpha_2} + \frac{\beta_1}{A_1 A_2} \frac{\partial A_2}{\partial \alpha_1}, \quad (2.72)$$

$$k_{12} = \frac{A_2}{A_1} \frac{\partial}{\partial \alpha_1} \left(\frac{\beta_2}{A_2} \right) + \frac{A_1}{A_2} \frac{\partial}{\partial \alpha_2} \left(\frac{\beta_1}{A_1} \right), \quad (2.73)$$

where β_1 and β_2 are angles given by

$$\beta_1 = \frac{u_1}{R_1} - \frac{1}{A_1} \frac{\partial u_3}{\partial \alpha_1}, \quad (2.74)$$

$$\beta_2 = \frac{u_2}{R_2} - \frac{1}{A_2} \frac{\partial u_3}{\partial \alpha_2}. \quad (2.75)$$

2.3.2 Strain-Displacement Relations for Cylindrical Thin Shells

Using equations (2.29), (2.30), (2.35), (2.36) for A_1 and A_2 , and equations (2.33), (2.34), (2.37), (2.38) for R_1 and R_2 , strains in an elliptical or a circular cylindrical shell can be shown to be

$$\varepsilon_{11}^o = \frac{1}{A_1} \frac{\partial u_1}{\partial \alpha_1} + \frac{u_3}{R_1}, \quad (2.76)$$

$$\varepsilon_{22}^o = \frac{\partial u_2}{\partial \alpha_2}, \quad (2.77)$$

$$\varepsilon_{12}^o = \frac{1}{A_1} \frac{\partial u_2}{\partial \alpha_1} + \frac{\partial u_1}{\partial \alpha_2}, \quad (2.78)$$

$$k_{11} = \frac{1}{A_1} \left\{ \frac{\partial}{\partial \alpha_1} \left(\frac{u_1}{R_1} \right) - \frac{\partial}{\partial \alpha_1} \left(\frac{1}{A_1} \frac{\partial u_3}{\partial \alpha_1} \right) \right\}, \quad (2.79)$$

$$k_{22} = -\frac{\partial^2 u_3}{\partial \alpha_2^2}, \quad (2.80)$$

$$k_{12} = \frac{1}{R_1} \frac{\partial u_1}{\partial \alpha_2} - \frac{2}{A_1} \frac{\partial^2 u_3}{\partial \alpha_2 \partial \alpha_1}, \quad (2.81)$$

$$\beta_1 = \frac{u_1}{R_1} - \frac{1}{A_1} \frac{\partial u_3}{\partial \alpha_1}, \quad (2.82)$$

$$\beta_2 = -\frac{\partial u_3}{\partial \alpha_2}. \quad (2.83)$$

2.3.3 Strain-Displacement Relations for Ellipsoidal (also Spheroidal) Thin Shells

Using equations (2.49), (2.50), (2.55), (2.56) for A_1 and A_2 , and equations (2.53), (2.54), (2.57), (2.58) for R_1 and R_2 , strains in an ellipsoidal and also spheroidal shell are found as:

$$\varepsilon_{11}^o = \frac{1}{A_1} \frac{\partial u_1}{\partial \alpha_1} + \frac{u_2}{A_1 A_2} \frac{\partial A_1}{\partial \alpha_2} + \frac{u_3}{R_1}, \quad (2.84)$$

$$\varepsilon_{22}^o = \frac{1}{A_2} \frac{\partial u_2}{\partial \alpha_2} + \frac{u_1}{A_1 A_2} \frac{\partial A_2}{\partial \alpha_1} + \frac{u_3}{R_2}, \quad (2.85)$$

$$\varepsilon_{12}^o = \frac{A_2}{A_1} \frac{\partial}{\partial \alpha_1} \left(\frac{u_2}{A_2} \right) + \frac{A_1}{A_2} \frac{\partial}{\partial \alpha_2} \left(\frac{u_1}{A_1} \right), \quad (2.86)$$

$$k_{11} = \frac{1}{A_1} \frac{\partial}{\partial \alpha_1} \left(\frac{u_1}{R_1} - \frac{1}{A_1} \frac{\partial u_3}{\partial \alpha_1} \right) + \frac{\left(\frac{u_2}{R_2} - \frac{1}{A_2} \frac{\partial u_3}{\partial \alpha_2} \right) \partial A_1}{A_1 A_2 \partial \alpha_2}, \quad (2.87)$$

$$k_{22} = \frac{1}{A_2} \frac{\partial}{\partial \alpha_2} \left(\frac{u_2}{R_2} - \frac{1}{A_2} \frac{\partial u_3}{\partial \alpha_2} \right) + \frac{\left(\frac{u_1}{R_1} - \frac{1}{A_1} \frac{\partial u_3}{\partial \alpha_1} \right) \partial A_2}{A_1 A_2 \partial \alpha_1}, \quad (2.88)$$

$$k_{12} = \frac{A_2}{A_1} \frac{\partial}{\partial \alpha_1} \left(\frac{\frac{u_2}{R_2} - \frac{1}{A_2} \frac{\partial u_3}{\partial \alpha_2}}{A_2} \right) + \frac{A_1}{A_2} \frac{\partial}{\partial \alpha_2} \left(\frac{\frac{u_1}{R_1} - \frac{1}{A_1} \frac{\partial u_3}{\partial \alpha_1}}{A_1} \right), \quad (2.89)$$

$$\beta_1 = \frac{u_1}{R_1} - \frac{1}{A_1} \frac{\partial u_3}{\partial \alpha_1}, \quad (2.90)$$

$$\beta_2 = \frac{u_2}{R_2} - \frac{1}{A_2} \frac{\partial u_3}{\partial \alpha_2}. \quad (2.91)$$

Note that, all of these strain – displacement relationships are used in strain and kinetic energy expressions of shells to develop suitable required finite element models.



CHAPTER THREE

SOLUTION PROCEDURE

In this chapter, solution procedure is explained and presented. Finite element solution technique is applied to achieve the result. Firstly, strain (potential) and kinetic energies are derived, and then ring elements are used to complete the finite element solution procedure.

3.1 STRAIN AND KINETIC ENERGY EXPRESSIONS FOR THIN SHELLS

For formulating the shell vibration problem by the help of the finite element method, energy expressions are required. Now, strain (potential) and kinetic energy expressions can be derived using the strain – displacement relations given in the preceding chapter.

3.1.1 Strain Energy

The strain energy stored in an infinitesimal element that is acted on by stresses σ_{ij} is (Soedel, 1993)

$$dP = \frac{1}{2} (\sigma_{11}\epsilon_{11} + \sigma_{22}\epsilon_{22} + \sigma_{12}\epsilon_{12} + \sigma_{13}\epsilon_{13} + \sigma_{23}\epsilon_{23} + \sigma_{33}\epsilon_{33}) dV. \quad (3.1)$$

As noted before in equations (2.62) to (2.64), according to Love simplifications, the last three terms in equation (3.1) can be neglected. Integrating this equation over the volume of the shell gives the total strain energy as

$$P = \int \int \int_{\alpha_1 \alpha_2 \alpha_3} \left\{ \frac{1}{2} (\sigma_{11} \varepsilon_{11} + \sigma_{22} \varepsilon_{22} + \sigma_{12} \varepsilon_{12}) \right\} dV, \quad (3.2)$$

where the infinitesimal volume dV is given by

$$dV = A_1 A_2 \left(1 + \frac{\alpha_3}{R_1} \right) \left(1 + \frac{\alpha_3}{R_2} \right) d\alpha_1 d\alpha_2 d\alpha_3, \quad (3.3)$$

and neglecting the $\frac{\alpha_3}{R_1}$, $\frac{\alpha_3}{R_2}$ terms, P becomes

$$P = \int \int \int_{\alpha_1 \alpha_2 \alpha_3} \left\{ \frac{1}{2} (\sigma_{11} \varepsilon_{11} + \sigma_{22} \varepsilon_{22} + \sigma_{12} \varepsilon_{12}) \right\} A_1 A_2 d\alpha_1 d\alpha_2 d\alpha_3. \quad (3.4)$$

According to the combination of Hooke's Law and Love simplification, the stress terms become (Soedel, 1993)

$$\sigma_{11} = \frac{E}{1-\mu^2} \left[\varepsilon_{11}^o + \mu \varepsilon_{22}^o + \alpha_3 (k_{11} + \mu k_{22}) \right], \quad (3.5)$$

$$\sigma_{22} = \frac{E}{1-\mu^2} \left[\varepsilon_{22}^o + \mu \varepsilon_{11}^o + \alpha_3 (k_{22} + \mu k_{11}) \right], \quad (3.6)$$

$$\sigma_{12} = G (\varepsilon_{12}^o + \alpha_3 k_{12}). \quad (3.7)$$

Here; μ is the *Poisson's ratio*, E is the *modulus of elasticity* and G is the *shear modulus*, where

$$G = \frac{E}{2(1+\mu)}. \quad (3.8)$$

Substituting equations (3.5) to (3.7) and equations (2.65) to (2.67) into equation (3.4), gives

$$P = \int \int \int_{\alpha_1 \alpha_2 \alpha_3} \left\{ \frac{1}{2} \left[\begin{aligned} &\frac{E}{1-\mu^2} [\varepsilon_{11}^o + \mu\varepsilon_{22}^o + \alpha_3(k_{11} + \mu k_{22})] (\varepsilon_{11}^o + \alpha_3 k_{11}) \\ &+ \frac{E}{1-\mu^2} [\varepsilon_{22}^o + \mu\varepsilon_{11}^o + \alpha_3(k_{22} + \mu k_{11})] (\varepsilon_{22}^o + \alpha_3 k_{22}) \\ &+ G(\varepsilon_{12}^o + \alpha_3 k_{12}) (\varepsilon_{12}^o + \alpha_3 k_{12}) \end{aligned} \right] \right\} A_1 A_2 d\alpha_1 d\alpha_2 d\alpha_3. \quad (3.9)$$

If this expression is integrated over the thickness of the shell from $-h/2$ to $h/2$, this gives

$$P = \int \int \int_{\alpha_1 \alpha_2 -h/2}^{h/2} \left\{ \frac{1}{2} \left[\begin{aligned} &\frac{E}{1-\mu^2} [\varepsilon_{11}^o + \mu\varepsilon_{22}^o + \alpha_3(k_{11} + \mu k_{22})] (\varepsilon_{11}^o + \alpha_3 k_{11}) \\ &+ \frac{E}{1-\mu^2} [\varepsilon_{22}^o + \mu\varepsilon_{11}^o + \alpha_3(k_{22} + \mu k_{11})] (\varepsilon_{22}^o + \alpha_3 k_{22}) \\ &+ G(\varepsilon_{12}^o + \alpha_3 k_{12}) (\varepsilon_{12}^o + \alpha_3 k_{12}) \end{aligned} \right] \right\} A_1 A_2 d\alpha_1 d\alpha_2 d\alpha_3, \quad (3.10)$$

and arranging this term gives the strain energy as

$$P = \frac{1}{2} \int \int_{\alpha_1 \alpha_2} \left\{ \begin{aligned} &K \left[\varepsilon_{11}^{o2} + 2\mu\varepsilon_{11}^o\varepsilon_{22}^o + \varepsilon_{22}^{o2} + \frac{1-\mu}{2} \varepsilon_{12}^{o2} \right] \\ &+ D \left[k_{11}^2 + 2\mu k_{11}k_{22} + k_{22}^2 + \frac{1-\mu}{2} k_{12}^2 \right] \end{aligned} \right\} A_1 A_2 d\alpha_1 d\alpha_2, \quad (3.11)$$

where K is named *membrane stiffness* and D is named *bending stiffness*. K and D are given by

$$K = \frac{Eh}{1-\mu^2}, \quad (3.12)$$

$$D = \frac{Eh^3}{12(1-\mu^2)}. \quad (3.13)$$

Equation (3.11) is required expressing for the strain energy. If the membrane (ε_{ij}^e) and bending (k_{ij}) strains are substituted in equation (3.11), the strain energy can be expressed in terms of shell displacements.

This is a general strain energy expression for any shape of shell. If equations (2.76) to (2.81) and equations (2.29), (2.30) are substituted into equation (3.11), strain energy for an elliptical cylindrical shell can be obtained. And if equations (2.84) to (2.89) and equations (2.49), (2.50) are substituted into equation (3.11), strain energy for an ellipsoidal shell can be obtained. Note that equations (2.35), (2.36) are valid for circular cylindrical and (2.55), (2.56) are for spheroidal shells.

3.1.2 Kinetic Energy

Kinetic energy of one infinitesimal element is given by (Soedel, 1993)

$$dT = \frac{1}{2} \rho (\dot{U}_1^2 + \dot{U}_2^2 + \dot{U}_3^2) dV. \quad (3.14)$$

Substituting equations (2.59) to (2.61) into equation (3.14) and integrating over the volume of the shell gives

$$T = \frac{1}{2} \rho \int_{\alpha_1} \int_{\alpha_2} \int_{\alpha_3} \left[\dot{u}_1^2 + \dot{u}_2^2 + \dot{u}_3^2 + \alpha_3^2 (\dot{\beta}_1^2 + \dot{\beta}_2^2) \right] A_1 A_2 \left(1 + \frac{\alpha_3}{R_1} \right) \left(1 + \frac{\alpha_3}{R_2} \right) d\alpha_1 d\alpha_2 d\alpha_3. \quad (3.15)$$

For thin shells, the quotients $\frac{\alpha_3}{R_1}$ and $\frac{\alpha_3}{R_2}$ can be neglected. Then, integrating over the shell thickness of the shell ($\alpha_3 = -h/2$ to $\alpha_3 = h/2$) gives the kinetic energy expression for any shape of shell.

$$T = \frac{1}{2} \rho h \int \int_{\alpha_1 \alpha_2} \left[\dot{u}_1^2 + \dot{u}_2^2 + \dot{u}_3^2 + \frac{h^2}{12} (\dot{\beta}_1^2 + \dot{\beta}_2^2) \right] A_1 A_2 d\alpha_1 d\alpha_2. \quad (3.16)$$

If equations (2.82), (2.83) are substituted into equation (3.16), kinetic energy of an elliptical and also a circular cylindrical shell can be obtained. And if equations (2.90), (2.91) are substituted into equation (3.16), kinetic energy of an ellipsoidal and a spheroidal shell can be obtained as well.

3.2 RING ELEMENTS FOR CYLINDRICAL AND SPHEROIDAL SHELLS

For analyzing the vibration problems of cylindrical or spheroid thin shells, finite element method will be used here. The strain and kinetic energies are reformulated in a matrix form for application of this solution technique. For α_1 direction, a sinusoidal function will be used and for the α_2 direction, a polynomial function will be used for representing the shell displacements. This type of finite element is called *ring element* used for axisymmetric thin shells of revolution in this study.

3.2.1 Ring Element Technique Used for Finite Element Modeling

The displacement functions that will be used in formulating the finite elements are (Soedel, 1993)

$$u_1(\alpha_2, \alpha_1) = U_1(\alpha_2) \sin n(\alpha_1 - \varphi), \quad (3.17)$$

$$u_2(\alpha_2, \alpha_1) = U_2(\alpha_2) \cos n(\alpha_1 - \varphi), \quad (3.18)$$

$$u_3(\alpha_2, \alpha_1) = U_3(\alpha_2) \cos n(\alpha_1 - \varphi), \quad (3.19)$$

where U_1 , U_2 and U_3 are the polynomial functions in α_2 . u_1 and u_2 displacements are tangential to α_1 and α_2 directions respectively. And u_3 is in the direction of the surface normal (see Fig. 3.1 and 3.2).

$$u_1 = (a_1 + a_2\alpha_2 + a_3\alpha_2^2 + a_4\alpha_2^3) \sin n(\alpha_1 - \varphi), \quad (3.20)$$

$$u_2 = (a_5 + a_6\alpha_2 + a_7\alpha_2^2 + a_8\alpha_2^3) \cos n(\alpha_1 - \varphi), \quad (3.21)$$

$$u_3 = (a_9 + a_{10}\alpha_2 + a_{11}\alpha_2^2 + a_{12}\alpha_2^3) \cos n(\alpha_1 - \varphi), \quad (3.22)$$

Equations (3.17) to (3.19) can be written in matrix form as

$$u_1 = \begin{bmatrix} 1 & \alpha_2 & \alpha_2^2 & \alpha_2^3 & 0 & 0 & 0 & 0 & 0 & 0 & 0 & 0 & 0 \end{bmatrix} \begin{bmatrix} a_1 \\ a_2 \\ a_3 \\ a_4 \\ a_5 \\ a_6 \\ a_7 \\ a_8 \\ a_9 \\ a_{10} \\ a_{11} \\ a_{12} \end{bmatrix} \sin n(\alpha_1 - \varphi), \quad (3.23)$$

$$u_2 = \begin{bmatrix} 0 & 0 & 0 & 0 & 1 & \alpha_2 & \alpha_2^2 & \alpha_2^3 & 0 & 0 & 0 & 0 & 0 \end{bmatrix} \begin{bmatrix} a_1 \\ a_2 \\ a_3 \\ a_4 \\ a_5 \\ a_6 \\ a_7 \\ a_8 \\ a_9 \\ a_{10} \\ a_{11} \\ a_{12} \end{bmatrix} \cos n(\alpha_1 - \varphi), \quad (3.24)$$

$$u_3 = \begin{bmatrix} 0 & 0 & 0 & 0 & 0 & 0 & 0 & 0 & 0 & 1 & \alpha_2 & \alpha_2^2 & \alpha_2^3 \end{bmatrix} \begin{bmatrix} a_1 \\ a_2 \\ a_3 \\ a_4 \\ a_5 \\ a_6 \\ a_7 \\ a_8 \\ a_9 \\ a_{10} \\ a_{11} \\ a_{12} \end{bmatrix} \cos n(\alpha_1 - \varphi), \quad (3.25)$$

General basic finite elements of the cylindrical and spheroid shells are shown in Figures 3.1 and 3.2. Terms of s_k and s_{k+1} are the general α_2 measures for any ring element.

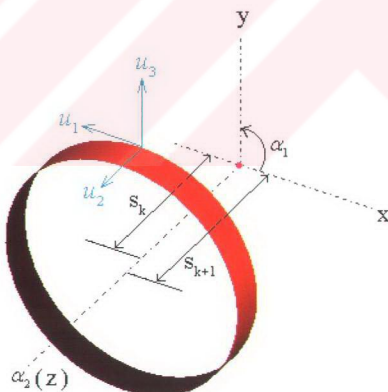


Figure 3.1 One ring finite element for circular cylinder.

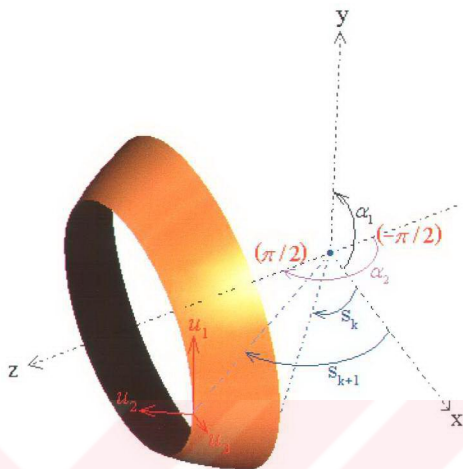


Figure 3.2 One ring finite element for spheroid.

$$\begin{bmatrix} (U_1)_k \\ \left(\frac{\partial U_1}{\partial a_2}\right)_k \\ (U_2)_k \\ \left(\frac{\partial U_2}{\partial a_2}\right)_k \\ (U_3)_k \\ \left(\frac{\partial U_3}{\partial a_2}\right)_k \\ (U_1)_{k+1} \\ \left(\frac{\partial U_2}{\partial a_2}\right)_{k+1} \\ (U_2)_{k+1} \\ \left(\frac{\partial U_2}{\partial a_2}\right)_{k+1} \\ (U_3)_{k+1} \\ \left(\frac{\partial U_3}{\partial a_2}\right)_{k+1} \end{bmatrix} = \begin{bmatrix} 1 & s_k & s_k^2 & s_k^3 & 0 & 0 & 0 & 0 & 0 & 0 & 0 & 0 \\ 0 & 1 & 2s_k & 3s_k^2 & 0 & 0 & 0 & 0 & 0 & 0 & 0 & 0 \\ 0 & 0 & 0 & 0 & 1 & s_k & s_k^2 & s_k^3 & 0 & 0 & 0 & 0 \\ 0 & 0 & 0 & 0 & 0 & 1 & 2s_k & 3s_k^2 & 0 & 0 & 0 & 0 \\ 0 & 0 & 0 & 0 & 0 & 0 & 0 & 0 & 1 & s_k & s_k^2 & s_k^3 \\ 0 & 0 & 0 & 0 & 0 & 0 & 0 & 0 & 0 & 1 & 2s_k & 3s_k^2 \\ 1 & s_{k+1} & s_{k+1}^2 & s_{k+1}^3 & 0 & 0 & 0 & 0 & 0 & 0 & 0 & 0 \\ 0 & 1 & 2s_{k+1} & 3s_{k+1}^2 & 0 & 0 & 0 & 0 & 0 & 0 & 0 & 0 \\ 0 & 0 & 0 & 0 & 1 & s_{k+1} & s_{k+1}^2 & s_{k+1}^3 & 0 & 0 & 0 & 0 \\ 0 & 0 & 0 & 0 & 0 & 1 & 2s_{k+1} & 3s_{k+1}^2 & 0 & 0 & 0 & 0 \\ 0 & 0 & 0 & 0 & 0 & 0 & 0 & 0 & 1 & s_{k+1} & s_{k+1}^2 & s_{k+1}^3 \\ 0 & 0 & 0 & 0 & 0 & 0 & 0 & 0 & 0 & 1 & 2s_{k+1} & 3s_{k+1}^2 \end{bmatrix} \begin{bmatrix} a_1 \\ a_2 \\ a_3 \\ a_4 \\ a_5 \\ a_6 \\ a_7 \\ a_8 \\ a_9 \\ a_{10} \\ a_{11} \\ a_{12} \end{bmatrix} \quad (3.26)$$

Briefly, this can be rewritten as

$$\mathbf{U} = \mathbf{C} \mathbf{a}, \quad (3.27)$$

and

$$\mathbf{a} = \mathbf{C}^{-1} \mathbf{U}. \quad (3.28)$$

By substituting equation (3.28) into equations (3.23) to (3.25), one can reach u_1 , u_2 and u_3 . And if these u_1 , u_2 and u_3 displacement equations are used in equation (3.11), the strain energy for a single ring element will be of the form

$$P = \frac{1}{2} \mathbf{U}^T \mathbf{C}^{-T} \int_0^{2\pi} \int_{s_1}^{s_1+1} [\mathbf{Q}(\alpha_1, \alpha_2, n)] d\alpha_1 d\alpha_2 \mathbf{C}^{-1} \mathbf{U}, \quad (3.29)$$

Proceeding similarly as equation (3.16), it can be shown that the kinetic energy also for a single ring element is in the form

$$T = \frac{1}{2} \rho h \dot{\mathbf{U}}^T \mathbf{C}^{-T} \int_0^{2\pi} \int_{s_1}^{s_1+1} [\mathbf{S}(\alpha_1, \alpha_2, n)] d\alpha_1 d\alpha_2 \mathbf{C}^{-1} \dot{\mathbf{U}}. \quad (3.30)$$

As it is known generally the potential and kinetic energy formulas are respectively

$$P = \frac{1}{2} \mathbf{U}^T \mathbf{k} \mathbf{U}, \quad (3.31)$$

$$T = \frac{1}{2} \dot{\mathbf{U}}^T \mathbf{m} \dot{\mathbf{U}}. \quad (3.32)$$

By the help of these forms, the stiffness and mass matrices for a structural element appear as,

$$\mathbf{k} = \mathbf{C}^{-T} \int_0^{2\pi} \int_{s_2}^{s_1} [\mathbf{Q}(\alpha_1, \alpha_2, n)] d\alpha_1 d\alpha_2 \mathbf{C}^{-1}, \quad (3.33)$$

$$\mathbf{m} = \rho h \mathbf{C}^{-T} \int_0^{2\pi} \int_{s_2}^{s_1} [\mathbf{S}(\alpha_1, \alpha_2, n)] d\alpha_1 d\alpha_2 \mathbf{C}^{-1}. \quad (3.34)$$

These matrices are for one single ring element. To find the whole mass and stiffness matrices for the complete shell geometry, these local ring elements are assembled into global matrices by connecting the circular edges of the elements end to end. This procedure is accomplished by satisfying the displacement continuity at the edge connections. In other words, the displacements and their derivatives must be same at the circular edge connections, because one edge is shared by two successive ring elements. Hence, for getting the entire (total) stiffness and mass matrices, the displacement terms at these shared edges are summed for each successive element's matrix.

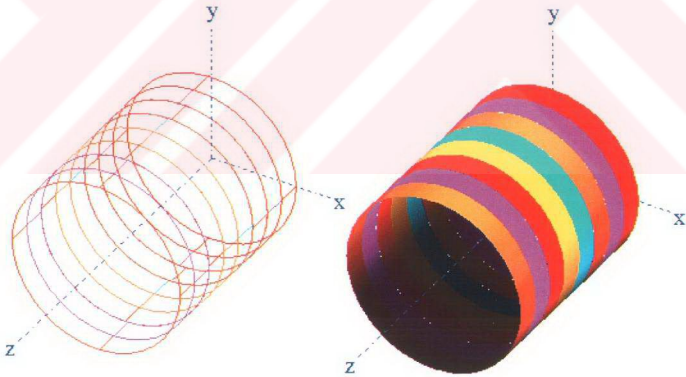


Figure 3.3 The whole finite element model for circular cylinder.

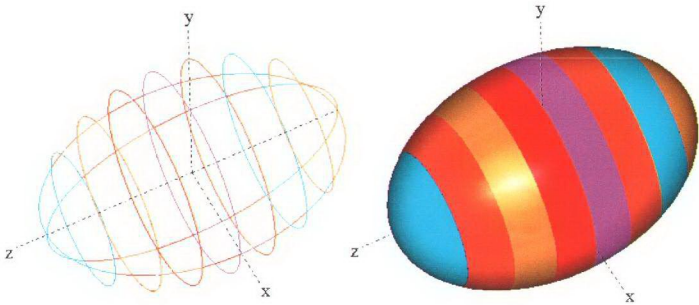


Figure 3.4 The whole finite element model for spheroid.

To derive the equation of motion of a structure for free vibration, Lagrange equations can be used. The Lagrange equations are given by

$$\frac{d}{dt} \left\{ \frac{\partial L}{\partial \dot{U}} \right\} - \frac{\partial L}{\partial U} + \frac{\partial R}{\partial \dot{U}} = 0, \quad (3.35)$$

where

$$L = T - P \quad (3.36)$$

is called the Lagrangian function, T is kinetic energy, P is the potential energy, R is the dissipation function, U is the displacement and \dot{U} is the velocity. As any dissipation is not considered here (such as damping), the dissipation function R is neglected. Therefore the Lagrange function reduces to

$$\frac{d}{dt} \left\{ \frac{\partial L}{\partial \dot{U}} \right\} - \frac{\partial L}{\partial U} = 0. \quad (3.37)$$

Lagrangian is

$$L = \frac{1}{2}(m\dot{U}^2 - kU^2). \quad (3.38)$$

By substituting L into (3.37) the equation of motion is obtained as

$$m\ddot{U} + kU = 0 \quad (3.39)$$

If a harmonically time dependency ($U = \hat{U}e^{i\omega t}$) is assumed for displacement function as a solution, then equation has the form

$$(k - \omega^2 m)U = 0. \quad (3.40)$$

In matrix form

$$(\mathbf{k}_{\text{total}} - \omega^2 \mathbf{m}_{\text{total}}) \mathbf{U} = 0. \quad (3.41)$$

By a simple arrangement, equation (3.41) turns to be a typical eigenvalue problem:

$$(\mathbf{m}^{-1} \mathbf{k}_{\text{total}} - \omega^2 \mathbf{I}) \mathbf{U} = 0. \quad (3.42)$$

If this eigenvalue problem is solved then the radian frequency values which give natural frequencies of the structure can be found.

3.3 APPROXIMATE RING ELEMENTS FOR ELLIPTIC AND ELLIPSOIDAL SHELLS

When constructing the finite element model of elliptical and ellipsoidal thin shells, it is assumed that the displacement functions (3.17) to (3.19) can be used also for elliptical and ellipsoidal ring elements. Although these functions are valid for axisymmetric shells of revolution, it is assumed that these can be used for asymmetric structures. By this assumption, the solution procedure is performed in the

same way with circular cylindrical and spheroidal shells. In other words, the equations given in Chapter 3 are also used for elliptical and ellipsoidal thin shells.

The strain – displacement equations of elliptic cylindrical and ellipsoidal thin shells are used in energy expressions during the finite element modeling procedure. And the geometric parameters, a and b are different from each other. Only these differences exist comparing to section 3.2. The solution procedure given in section 3.2 is also valid for section 3.3.



CHAPTER FOUR

NUMERICAL RESULTS AND COMPARATIVE EXAMPLES

In this chapter, numerical results for some thin shell structures are given. And the results for these shell structures are compared with the results of a commercial software package IDEAS.

4.1 RESULTS FOR SOME CYLINDRICAL AND SPHEROIDAL THIN SHELL STRUCTURES

To find the fundamental natural frequencies of some cylindrical and spheroidal thin shell structures, MATLAB programmable “m” files were written. For the same shell structures and boundary conditions, both MATLAB programs and well-known commercial cad/cam software I-DEAS found the frequencies. The results were compared to check the reliability of the written programs and the calculations derived during the entire study.

The structures, its boundary conditions, geometric parameters, material properties and meshed drawings in IDEAS software are depicted by Figures 4.1 – 4.4. And note that typical *structural steel* was considered during the analysis procedures.

The MATLAB program names (“m” file names) and the results are given by Tables 4.1 – 4.4 and Figures 4.1 – 4.4. These are the fundamental natural frequencies of each of the related shell structure. As it can be seen from the tables, the results found by the MATLAB programs are satisfactory close to the IDEAS’ ones.

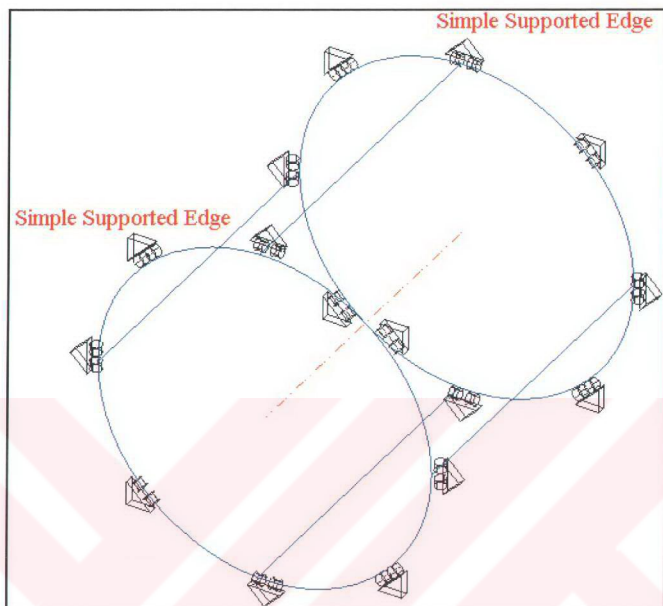


Figure 4.1 The simple supported cylinder at both edges that lets axial motion (File1.m). ($a=b=60$ mm, cylinder length $L=120$ mm, $h=3$ mm, $\mu=0.3$, $E=206$ GPa, $\rho=7860$ kg/m³)

As it can be seen from the Table 4.1, exceptionally there is also a theoretical exact result is given (El-Mously, 2003) for a better comparison opportunity.

Table 4.1 Comparison of natural frequencies obtained by different solution sources for Fig.4.1. (circumferential mode number, $n_2=3$)

	File1.m	I-DEAS	Exact Result
ω (Hz)	3481	3429	3414

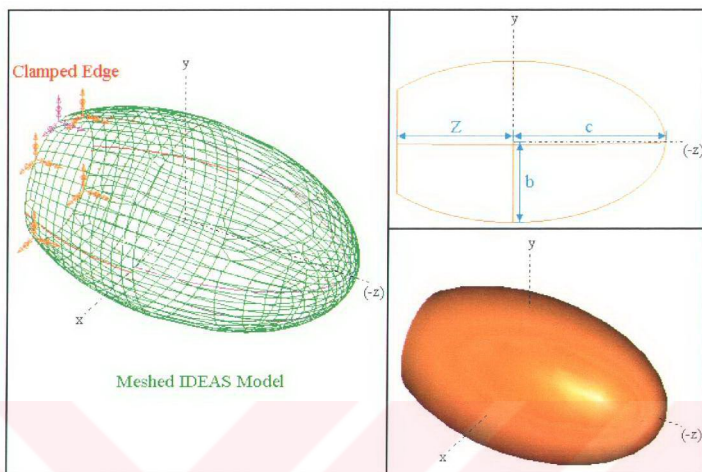


Figure 4.2 The spheroidal thin shell clamped at cut edge (File2.m). ($a=b=45$ mm, $c=85$ mm, length $Z=65$ mm, $h=3.5$ mm, $\mu=0.3$, $E=206$ GPa, $\rho=7860$ kg/m³)

Table 4.2 Comparison of natural frequencies obtained by different solution sources for Fig.4.2. (circumferential mode number, $n_1=1$)

	File2.m	I-DEAS
w (Hz)	1844	1815

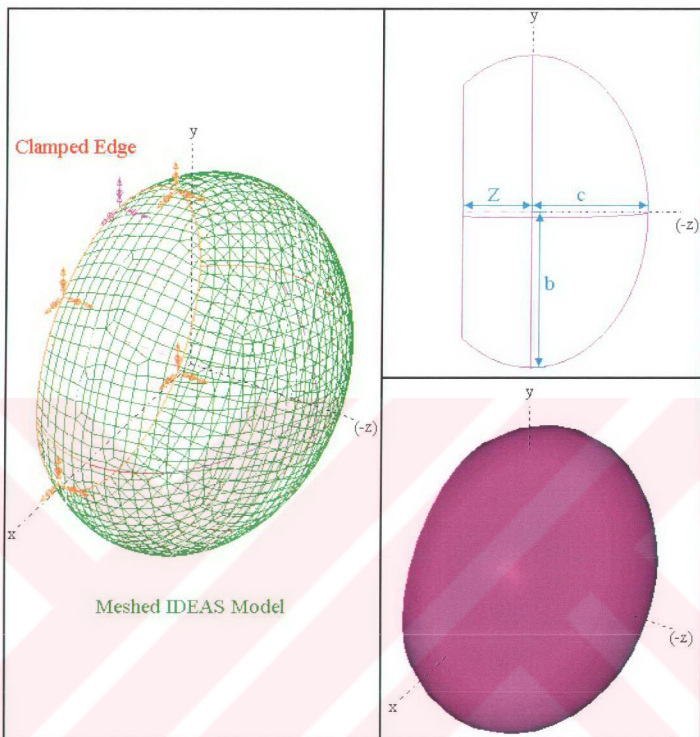


Figure 4.3 The spheroidal thin shell clamped at cut edge (File3.m). ($a=b=80$ mm, $c=60$ mm, length $Z=35$ mm, $h=3.5$ mm, $\mu=0.3$, $E=206$ GPa, $\rho=7860$ kg/m³)

Table 4.3 Comparison of natural frequencies obtained by different solution sources for Fig.4.3. (circumferential mode number, $n_1=1$)

	File3.m	I-DEAS
w (Hz)	3350	3308

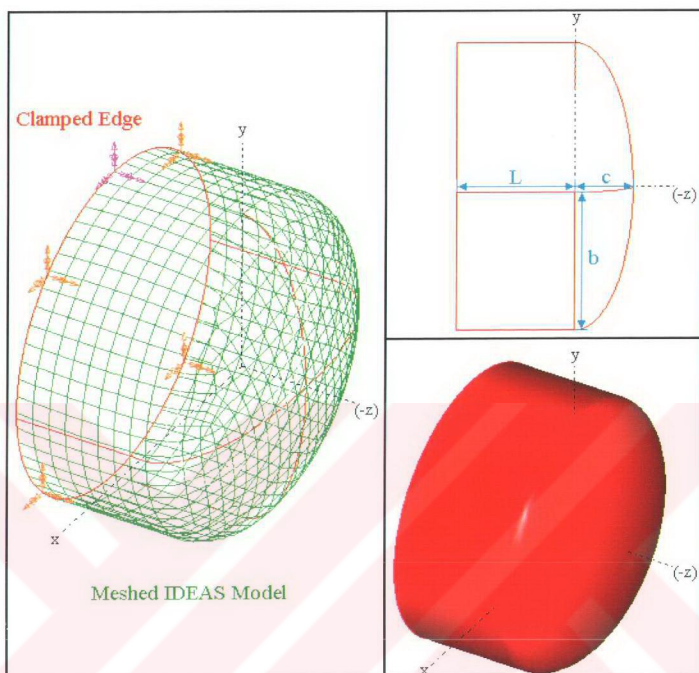


Figure 4.4 The thin shell formed by the combination of a half spheroidal and a circular cylindrical thin shell which is clamped at cylindrical edge (File4.m).
 ($a=b=75$ mm, $c=30$ mm, cylinder length $L=60$ mm, $h=3.5$ mm, $\mu=0.3$, $E=206$ GPa,
 $\rho=7860$ kg/m³)

Table 4.4 Comparison of natural frequencies obtained by different solution sources for Fig. 4.4. (circumferential mode numbers of spheroid cap and cylinder, $n_1=1$, $n_2=1$)

	File4.m	I-DEAS
w (Hz)	4582	4509

4.2 RESULTS FOR SOME ELLIPTICAL AND ELLIPSOIDAL THIN SHELL STRUCTURES

As indicated in section 4.1, some circular cylindrical and spheroidal shell examples with various boundary conditions were studied. The numerical results found by MATLAB programmes and IDEAS results are given and compared.

Now, a and b parameters are changed and these geometries are turned to be elliptical and ellipsoidal thin shell structures. Other geometric and material parameters are same with the structures depicted in Figures 4.1 – 4.4. The numerical results found by MATLAB are given at the below (Table 4.5) referring to Figures 4.1 – 4.4. The parameters are also given by Table 4.5.

Table 4.5 Fundamental natural frequencies for elliptical and ellipsoidal shells obtained by finite element programmes.

Filename	Geometric Parameters		Circumferential Mode	Fundamental Frequency (Hz)
	a (mm)	b (mm)		
File1.m	63	57	3	3617
File2.m	47	43	1	3410
File3.m	83	77	1	3925
File4.m	77	73	(1,1)	4877

CHAPTER FIVE

EXPERIMENT RESULTS

In this chapter, experimental setup and test results are presented. Firstly, the experiment procedure is described and then a comparison between the experimental and computational results is presented. The purpose of the test was to measure the first few natural frequencies of a compressor shell and compare the measurement with the predictions of the theory. The measured shell is made of a geometry which is a combination of an elliptical-like cylinder and an ellipsoidal-like cap. A similar figure is given by Fig. 5.2.

5.1 EXPERIMENTAL SETUP AND PROCEDURE

Test equipment connection can be depicted as in Fig. 5.1.

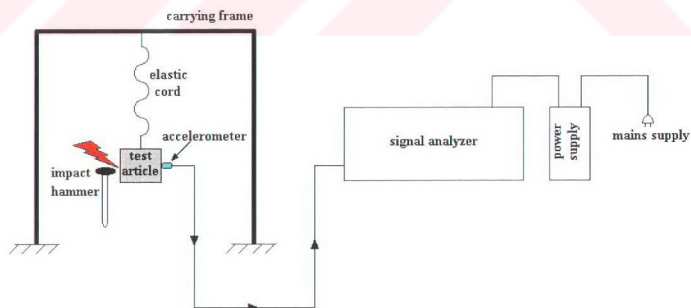


Figure 5.1 Schematic illustration of the test equipment connection.

During the experiment, a *dual channel portable signal analyzer (Brüel&Kjaer Type 2148)* which includes a *power supply (ZG 0199)*, and an *accelerometer (Brüel&Kjaer Type 4338)* were used as test instruments.

An elastic cord was used to satisfy the fully free boundary condition, by hanging the test article with the help of it. A carrying frame was used to hang the test article and an impact hammer was also used to give an impulsive excitation to the test article. These were the other assistant test components.

As the main goal of the test was to do frequency spectral analysis, firstly the *FFT Program* which is one of the signal analyzer's accessories was installed. After the installation the analyzer was ready for the experimental procedure. Then the connections of the test equipment were done carefully (see Fig. 5.1).

This test can be named as *impact hammer experiment* or in other words *impulse excitation test*. An impulsive excitation is a force that is applied for a very short, or infinitesimal, length of time. And an impulse applied to a system is the same as applying the initial condition of an initial velocity to that system. At the same time, the impulse response is also physically interpreted as the response to an initial velocity. Therefore if the test article (structure) is exposed to an impulsive excitation by an impact hammer stroke then it begins to vibrate with its natural modes, because the frequency solutions for an impulse excitation are the natural frequencies. So if the vibration of the structure is measured by an accelerometer and if the amplitudes are monitored in frequency domain, these natural frequencies reveal their selves by showing the peak values at these frequency values. By this way, these frequencies can be determined experimentally. This type of frequency based analysis is known as *frequency spectrum analysis* or *Fourier analysis*.

According to the procedure above; firstly the equipment connections were completed and the test structure was hanged, then an impact hammer was used to apply an impulse to the test structure. The experimental results were obtained and copied as a text file in a HD disk and could be plotted (see Fig. 5.3).

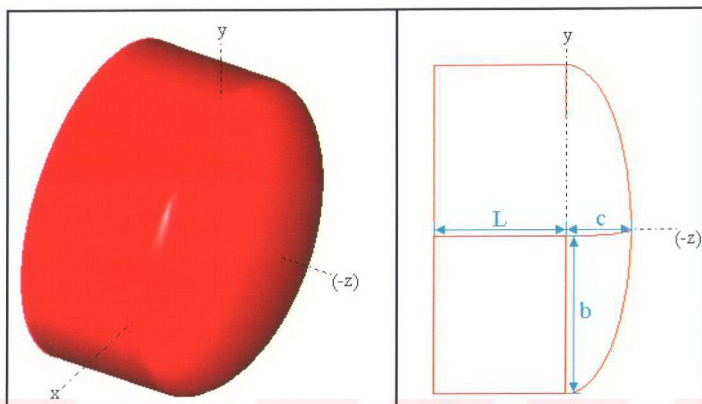


Figure 5.2 Thin shell structure wanted to be tested for fully free boundary condition.
 ($c=30$ mm, $L=60$ mm, $h=3.5$ mm, $\mu=0.3$, $E=206$ GPa, $\rho=7860$ kg/m³,
 $a=b=75$ mm for Model – I; $a=77$ mm, $b=73$ mm for Model – II)

Fig. 5.2 shows the structure for which the numerical results are calculated. As it is seen from the figure explanation there are two models, named as “Model – I” and “Model – II”. Model – I is formed by a combination of a circular cylinder and a spheroid cap, and Model – II is formed by a combination of elliptical cylinder and ellipsoidal cap. Results of the experiment and the comparison of these with the calculated ones are given by Fig. 5.3 and Table 5.1. “Free.m” is the file name of the MATLAB programme written for finding the numerical results and it is given by Appendix 1.

The test specimen has not the same shape with the Model – I, but they are similar shell structures. Hence, this similarity gives a chance to a comparative study. Despite the small physically shape difference between Model – I and the test structure, it can be seen that the experimental result supports the calculations. And for Model – I, the circumferential mode (1,1) gives a frequency near to zero which represents the rigid body motion. On the other hand Model – II is much more similar to the test specimen. The geometric parameters a , b are changed according to the test

structure's physical appearance. Because the tested structure has not a circular, but an elliptical like cross-section. Despite the geometric parameters are adapted according to the test structure's original shape, the calculated numerical results deviate much more from the experimental ones; whereas it is expected that the calculations (see Table 5.1) will agree with the experimental results in a better manner than the first case (Model – I). In addition, for rigid body motion circumferential mode numbers (1,1) does not give a frequency value of zero or in the vicinity of zero for Model – II. The obtained frequency for mode (1,1) is 463 Hz.

Although the numerical results of Model – I are completely true, this can not be said for Model – II. Because, a single harmonic function (sine or cosine) was used for representing the displacement function in the direction of a_1 in F.E.M given by Chapter 3. This type of harmonic function can only be valid for shells which have circular cross sections, but not completely true for axially asymmetric shells, like elliptical ones. When this model is used for elliptical thin shells, the results deviate from the reality. The more asymmetric the shell becomes, the more the result deviation will observed. But for small differences between a and b parameters, the model does not exaggeratedly reveal its error by means of the results.

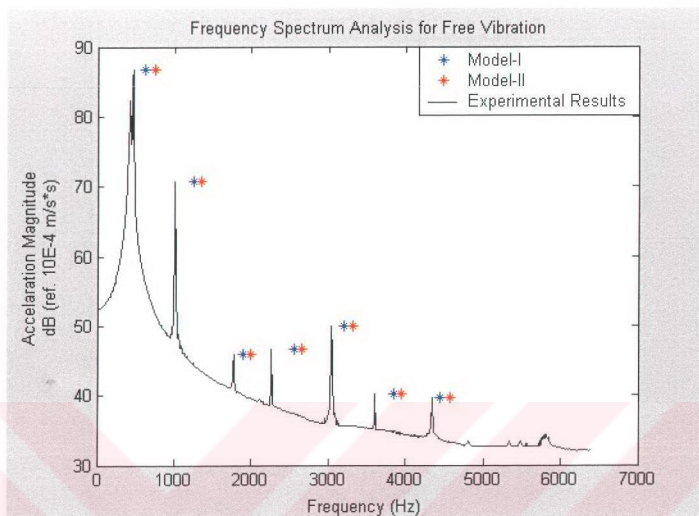


Figure 5.3 Comparison of numerical (Model-I & Model-II) and experimental results (circumferential mode numbers of numerical results for cap and cylinder are respectively (2,1), (3,1), (4,1), (5,1), (6,1), (7,1), (8,1)).

Table 5.1 Numerical presentation of Fig. 5.3.

	Model-I	Model-II	Experimental Res.
w_1 (Hz)	623	752	464
w_2 (Hz)	1250	1346	1008
w_3 (Hz)	1901	1998	1776
w_4 (Hz)	2556	2656	2264
w_5 (Hz)	3207	3312	3040
w_6 (Hz)	3843	3955	3600
w_7 (Hz)	4449	4568	4344

CHAPTER SIX

CONCLUSIONS

6.1 CONCLUSIONS

A theoretical and experimental study on finding the primary resonance frequencies of the circular and elliptical cylindrical, spheroidal and ellipsoidal thin shells is presented in the present thesis. Love theory (Soedel, 1993) has been used during the derivations of thin shell equations. None of any other simplifications or assumptions has been used during the derivations.

The Finite Element Method formed by ring elements has been used as the analysis method. By using the ring elements, one of the two curvilinear coordinates has been eliminated. This method gives an opportunity to simplify the modeling and calculating stage. The model was based on potential (strain) and kinetic energy expressions of the shell structures.

MATLAB software gives a great possibility to complicated matrix calculations and flexible programmable computer codes. Hence, numerical results have been calculated with the help of the programs (“m” files) which were constructed by the computer codes written in MATLAB – 6.1. The validity of the written programs has been proved by the comparison with a well – known commercial cad/cam software IDEAS. For the same thin shell geometries, very close results have been found by MATLAB programs and by IDEAS analysis. Besides this comparison, it has been observed that the numerical results satisfy the theoretical exact solutions (Soedel, 1993), (El-Mously, 2003).

Although the tested shell structure has not exactly the same shape -but similar- with the computed ones, the experimental and calculated results are seemed to be in an agreement, especially for Model – I.

As given in detail in Chapter 5, single harmonic displacement function used in finite element model does not give completely true numerical results for asymmetric elliptical and ellipsoidal thin shells. In the future studies, a more appropriate function will be used in the solution model to represent the α_1 dependent displacements on the ring element, for these types of asymmetric thin shells.



REFERENCES

- Akbulut, F. (1970). Vektörel analiz. İzmir: Ege Üniversitesi Matbaası.
- Donnell, L.H. (1976). Beams, Plates and Shells. New York: McGraw – Hill.
- El-Mously, M. (2003). Fundamental natural frequencies of thin cylindrical shells: a comparative study. Journal of Sound and Vibration, 264, 1167-1186.
- Kreyszig, E. (1959). Differential geometry. Toronto: University of Toronto Press.
- Kreyszig, E. (1993). Advanced engineering mathematics. (7th ed.). New York: John Wiley & Sons.
- Lipschutz, M.M. (1969). Theory and problems of differential geometry. New York: McGraw – Hill.
- Markus, S. (1988). The mechanics of vibrations of cylindrical shells. Elsevier Applied Mechanics.
- Soedel, W. (1976). Shells and plates loaded by dynamic moments with special attention to rotating point moments. Journal of Sound and Vibration, 48, 179-188.
- Soedel, W. (1993). Vibrations of shells and plates. (2nd ed.). New York: Marcel Dekker.

Thomas, G.B., & Finney, R.L. (1992). Calculus and analytic geometry – part 2. (8th ed.). New York: Addison-Wesley Publishing Company.



APPENDICES

APPENDIX 1: MatLab Codes of “Free.m” Programme.

```

clc;
clear;
SUBJECT=(' THIN SHELL VIBRATION ')
ATTENTION=(' Be sure that "additionalfile1.m", "additionalfile2.m",
"additionalfile3.m" and "additionalfile4.m" are in the same folder with "Free.m" ')

mu=input(' Poisson Ratio -> mu : ');
E=input(' Modulus of Elasticity(Pa) -> E : ');
ro=input(' Density of the Shell Material(kg/m^3) -> ro : ');
h=input(' Thickness of the Shell(m) -> h : ');
a=input(' x-Axis Geometric Parameter(m) -> a : ');
b=input(' y-Axis Geometric Parameter(m) -> b : ');
c=input(' z-Axis Geometric Parameter(m) -> c : ');
L=input(' Length of the Cylinder (m) -> L : ');
fii=0;
n1=input(' Circumferential Mode Number for Spheroid(also Ellipsoid) -> n1 : ');
n2=input(' Circumferential Mode Number for Cylinder -> n2 : ');

K=E*h/(1-mu^2);    %Membrane Stiffness (Pascal*meter)
D=E*h^3/12/(1-mu^2); %Bending Stiffness (Newton*meter)

syms a1 a2; %Curvilinear Coordinates

```



```

el_num=input(' Element Number for FEM of the Structural Parts -> el_num : ');
m=input(' Numeric Integral Parameter for Simpson Method -> m : ');

```

```

%Zkok=[1;a2;a2^2;a2^3];
%Z1=[Zkok',zeros(1,8)];
%Z2=[zeros(1,4),Zkok',zeros(1,4)];
%Z3=[zeros(1,8),Zkok'];
%Z=[Z1
%   Z2
%   Z3];

```

```

%u1=Z1*sin(n*(a1-fii));
%u2=Z2*cos(n*(a1-fii));
%u3=Z3*cos(n*(a1-fii));

```

```

%%%%%%%%%%%%%%%%%%%%%%%%%%%%%%%%%%%%%%%%%%%%%%%%%%%%%%%%%%
% NOTE THAT Ep11,Ep22,Ep12,beta1,beta2,k11,k22,k12 strain expressions are %
% included in additionalfile_1,2,3 and 4. %
%%%%%%%%%%%%%%%%%%%%%%%%%%%%%%%%%%%%%%%%%%%%%%%%%%%%%%%%%%

```

```

gamma=pi/2/el_num;
Kmat1=zeros(6*el_num+6);
Mmat1=zeros(6*el_num+6);

```

```

for i=1:1:el_num;
    o=0;
    p=2*pi;
    r=(i-1)*gamma+(-pi/2);
    s=i*gamma+(-pi/2);
    int_num=2*m;
    difference1=(p-o)/int_num;
    difference2=(s-r)/int_num;

```

```

C=[1,r,r^2,r^3,zeros(1,8)
  0,1,2*r,3*r^2,zeros(1,8)
  zeros(1,4),1,r,r^2,r^3,zeros(1,4)
  zeros(1,4),0,1,2*r,3*r^2,zeros(1,4)
  zeros(1,8),1,r,r^2,r^3
  zeros(1,8),0,1,2*r,3*r^2
  1,s,s^2,s^3,zeros(1,8)
  0,1,2*s,3*s^2,zeros(1,8)
  zeros(1,4),1,s,s^2,s^3,zeros(1,4)
  zeros(1,4),0,1,2*s,3*s^2,zeros(1,4)
  zeros(1,8),1,s,s^2,s^3
  zeros(1,8),0,1,2*s,3*s^2];

%/////////////////////////////////////////////////////////////////

odd=zeros(12,12);
even=zeros(12,12);
for j=1:2:int_num-1;
  a1=o+j*difference1;
  %-----
  odd1=zeros(12,12);
  even1=zeros(12,12);
  for j=1:2:int_num-1;
    a2=r+j*difference2;

    additionalfile1;

    A1=cos(a2)*sqrt((a*sin(a1))^2+(b*cos(a1))^2);
    A2=sqrt((a*sin(a2)*cos(a1))^2+(b*sin(a2)*sin(a1))^2+(c*cos(a2))^2);

    B=K*(Ep11*Ep11'+2*mu*Ep11*Ep22'+Ep22*Ep22'+(1-mu)/2
*Ep12*Ep12')*A1*A2 + D*(k11*k11'+2*mu*k11*k22'+k22*k22'+(1-mu)/2
*k12*k12')*A1*A2;

```

```

        odd1=odd1+B;
    end
    for j=2:2:int_num-2;
        a2=r+j*difference2;

        additionalfile1;

        A1=cos(a2)*sqrt((a*sin(a1))^2+(b*cos(a1))^2);
        A2=sqrt((a*sin(a2)*cos(a1))^2+(b*sin(a2)*sin(a1))^2+(c*cos(a2))^2);

        B=K*(Ep11*Ep11'+2*mu*Ep11*Ep22'+Ep22*Ep22'+(1-mu)/2
        *Ep12*Ep12')*A1*A2 + D*(k11*k11'+2*mu*k11*k22'+k22*k22'+(1-mu)/2
        *k12*k12')*A1*A2;

        even1=even1+B;
    end

    a2=r;yo=B;
    a2=s;yp=B;

    G=difference2/3*(yo+yp+4*odd1+2*even1);
    %-----
    odd=odd+G;
end
for j=2:2:int_num-2;
    a1=o+j*difference1;
    %-----
    odd1=zeros(12,12);
    even1=zeros(12,12);
    for j=1:2:int_num-1;
        a2=r+j*difference2;

```

```

additionalfile1;

A1=cos(a2)*sqrt((a*sin(a1))^2+(b*cos(a1))^2);
A2=sqrt((a*sin(a2)*cos(a1))^2+(b*sin(a2)*sin(a1))^2+(c*cos(a2))^2);

B=K*(Ep11*Ep11'+2*mu*Ep11*Ep22'+Ep22*Ep22'+(1-mu)/2
*Ep12*Ep12')*A1*A2 + D*(k11*k11'+2*mu*k11*k22'+k22*k22'+(1-mu)/2
*k12*k12')*A1*A2;

    odd1=odd1+B;
end
for j=2:2:int_num-2;
    a2=r+j*difference2;

additionalfile1;

A1=cos(a2)*sqrt((a*sin(a1))^2+(b*cos(a1))^2);
A2=sqrt((a*sin(a2)*cos(a1))^2+(b*sin(a2)*sin(a1))^2+(c*cos(a2))^2);

B=K*(Ep11*Ep11'+2*mu*Ep11*Ep22'+Ep22*Ep22'+(1-mu)/2
*Ep12*Ep12')*A1*A2 + D*(k11*k11'+2*mu*k11*k22'+k22*k22'+(1-mu)/2
*k12*k12')*A1*A2;

    even1=even1+B;
end

a2=r;yo=B;
a2=s;yp=B;
G=difference2/3*(yo+yp+4*odd1+2*even1);
%-----
even=even+G;
end

```

```

a1=o;xo=G;
a1=p;xp=G;

I=difference1/3*(xo+xp+4*odd+2*even);
%
-----
odd=zeros(12,12);
even=zeros(12,12);
for j=1:2:int_num-1;
    a1=o+j*difference1;
    %-----
    odd1=zeros(12,12);
    even1=zeros(12,12);
    for j=1:2:int_num-1;
        a2=r+j*difference2;

        additionalfile2;

        A1=cos(a2)*sqrt((a*sin(a1))^2+(b*cos(a1))^2);
        A2=sqrt((a*sin(a2)*cos(a1))^2+(b*sin(a2)*sin(a1))^2+(c*cos(a2))^2);

B=ro*h*(u1*u1'+u2*u2'+u3*u3'+h^2/12*(beta1*beta1'+beta2*beta2'))*A1*A2;

        odd1=odd1+B;
    end
end
for j=2:2:int_num-2;
    a2=r+j*difference2;
    additionalfile2;
    A1=cos(a2)*sqrt((a*sin(a1))^2+(b*cos(a1))^2);
    A2=sqrt((a*sin(a2)*cos(a1))^2+(b*sin(a2)*sin(a1))^2+(c*cos(a2))^2);

B=ro*h*(u1*u1'+u2*u2'+u3*u3'+h^2/12*(beta1*beta1'+beta2*beta2'))*A1*A2;

```

```

        even1=even1+B;
    end

    a2=r;yo=B;
    a2=s;yp=B;

    G=difference2/3*(yo+yp+4*odd1+2*even1);
    %-----
    odd=odd+G;
end
for j=2:2:int_num-2;
    a1=o+j*difference1;
    %-----
    odd1=zeros(12,12);
    even1=zeros(12,12);
    for j=1:2:int_num-1;
        a2=r+j*difference2;

        additionalfile2;

        A1=cos(a2)*sqrt((a*sin(a1))^2+(b*cos(a1))^2);
        A2=sqrt((a*sin(a2)*cos(a1))^2+(b*sin(a2)*sin(a1))^2+(c*cos(a2))^2);

B=ro*h*(u1*u1'+u2*u2'+u3*u3'+h^2/12*(beta1*beta1'+beta2*beta2'))*A1*A2;

        odd1=odd1+B;
    end
    for j=2:2:int_num-2;
        a2=r+j*difference2;

        additionalfile2;

```

```
A1=cos(a2)*sqrt((a*sin(a1))^2+(b*cos(a1))^2);
```

```
A2=sqrt((a*sin(a2)*cos(a1))^2+(b*sin(a2)*sin(a1))^2+(c*cos(a2))^2);
```

```
B=ro*h*(u1*u1'+u2*u2'+u3*u3'+h^2/12*(beta1*beta1'+beta2*beta2'))*A1*A2;
```

```
even1=even1+B;
```

```
end
```

```
a2=r;yo=B;
```

```
a2=s;yp=B;
```

```
G=difference2/3*(yo+yp+4*odd1+2*even1);
```

```
%-----
```

```
even=even+G;
```

```
end
```

```
a1=o;xo=G;
```

```
a1=p;xp=G;
```

```
II=difference1/3*(xo+xp+4*odd+2*even);
```

```
%
```

```
%%%%%%%%%%%%%%%%%%%%%%%%%%%%%%%%%%%%%%%%%%%%%%%%%%%%%%%%%%%%%%%%%%%%%%%%%
```

```
kk=(inv(C))*I*(inv(C));
```

```
mm=(inv(C))*II*(inv(C));
```

```
kg=zeros(6*el_num+6);
```

```
mg=zeros(6*el_num+6);
```

```
kg(6*i-5:6*i+6,6*i-5:6*i+6)=kk;
```

```
mg(6*i-5:6*i+6,6*i-5:6*i+6)=mm;
```

```
Kmat1=Kmat1+kg;
```

```
Mmat1=Mmat1+mg;
```



```

odd=zeros(12,12);
even=zeros(12,12);
for j=1:2:int_num-1;
    a1=o+j*difference1;
    %-----
    odd1=zeros(12,12);
    even1=zeros(12,12);
    for j=1:2:int_num-1;
        a2=r+j*difference2;

        additionalfile3;

        A1=sqrt((a*sin(a1))^2+(b*cos(a1))^2);
        A2=1;

        B=K*(Ep11*Ep11'+2*mu*Ep11*Ep22'+Ep22*Ep22'+(1-mu)/2
*Ep12*Ep12')*A1*A2 + D*(k11*k11'+2*mu*k11*k22'+k22*k22'+(1-mu)/2
*k12*k12')*A1*A2;

        odd1=odd1+B;
    end
end
for j=2:2:int_num-2;
    a2=r+j*difference2;

    additionalfile3;

    A1=sqrt((a*sin(a1))^2+(b*cos(a1))^2);
    A2=1;

    B=K*(Ep11*Ep11'+2*mu*Ep11*Ep22'+Ep22*Ep22'+(1-mu)/2
*Ep12*Ep12')*A1*A2 + D*(k11*k11'+2*mu*k11*k22'+k22*k22'+(1-mu)/2
*k12*k12')*A1*A2;

```

```

        even1=even1+B;
    end

    a2=r;yo=B;
    a2=s;yp=B;

    G=difference2/3*(yo+yp+4*odd1+2*even1);
    %-----
    odd=odd+G;
end
for j=2:2:int_num-2;
    a1=o+j*difference1;
    %-----
    odd1=zeros(12,12);
    even1=zeros(12,12);
    for j=1:2:int_num-1;
        a2=r+j*difference2;

        additionalfile3;

        A1=sqrt((a*sin(a1))^2+(b*cos(a1))^2);
        A2=1;

        B=K*(Ep11*Ep11'+2*mu*Ep11*Ep22'+Ep22*Ep22'+(1-mu)/2
        *Ep12*Ep12')*A1*A2 + D*(k11*k11'+2*mu*k11*k22'+k22*k22'+(1-mu)/2
        *k12*k12')*A1*A2;

        odd1=odd1+B;
    end
    for j=2:2:int_num-2;
        a2=r+j*difference2;

```

```

additionalfile3;

A1=sqrt((a*sin(a1))^2+(b*cos(a1))^2);
A2=1;

B=K*(Ep11*Ep11'+2*mu*Ep11*Ep22'+Ep22*Ep22'+(1-mu)/2
*Ep12*Ep12')*A1*A2 + D*(k11*k11'+2*mu*k11*k22'+k22*k22'+(1-mu)/2
*k12*k12')*A1*A2;

    even1=even1+B;
end

a2=r;yo=B;
a2=s;yp=B;

G=difference2/3*(yo+yp+4*odd1+2*even1);
%-----
even=even+G;
end
a1=o;xo=G;
a1=p;xp=G;

I=difference1/3*(xo+xp+4*odd+2*even);
%_____
odd=zeros(12,12);
even=zeros(12,12);
for j=1:2:int_num-1;
    a1=o+j*difference1;
    %-----
    odd1=zeros(12,12);
    even1=zeros(12,12);
    for j=1:2:int_num-1;

```

```

a2=r+j*difference2;

additionalfile4;

A1=sqrt((a*sin(a1))^2+(b*cos(a1))^2);
A2=1;

B=ro*h*(u1*u1'+u2*u2'+u3*u3'+h^2/12*(beta1*beta1'+beta2*beta2'))*A1*A2;

    odd1=odd1+B;
end
for j=2:2:int_num-2;
    a2=r+j*difference2;

    additionalfile4;

    A1=sqrt((a*sin(a1))^2+(b*cos(a1))^2);
    A2=1;

    B=ro*h*(u1*u1'+u2*u2'+u3*u3'+h^2/12*(beta1*beta1'+beta2*beta2'))*A1*A2;
    even1=even1+B;
end

a2=r;yo=B;
a2=s;yp=B;

G=difference2/3*(yo+yp+4*odd1+2*even1);
%-----
odd=odd+G;
end
for j=2:2:int_num-2;
    a1=o+j*difference1;

```

```

%-----
odd1=zeros(12,12);
even1=zeros(12,12);
for j=1:2:int_num-1;
    a2=r+j*difference2;

    additionalfile4;

    A1=sqrt((a*sin(a1))^2+(b*cos(a1))^2);
    A2=1;

B=ro*h*(u1*u1'+u2*u2'+u3*u3'+h^2/12*(beta1*beta1'+beta2*beta2'))*A1*A2;

    odd1=odd1+B;
end
for j=2:2:int_num-2;
    a2=r+j*difference2;

    additionalfile4;

    A1=sqrt((a*sin(a1))^2+(b*cos(a1))^2);
    A2=1;

B=ro*h*(u1*u1'+u2*u2'+u3*u3'+h^2/12*(beta1*beta1'+beta2*beta2'))*A1*A2;

    even1=even1+B;
end

a2=r;yo=B;
a2=s;yp=B;

G=difference2/3*(yo+yp+4*odd1+2*even1);

```

```

%-----
even=even+G;
end

a1=o;xo=G;
a1=p;xp=G;

II=difference1/3*(xo+xp+4*odd+2*even);
%_____
%////////////////////////////////////
kk=(inv(C))*I*(inv(C));
mm=(inv(C))*II*(inv(C));

kg=zeros(6*el_num+6);
mg=zeros(6*el_num+6);

kg(6*i-5:6*i+6,6*i-5:6*i+6)=kk;
mg(6*i-5:6*i+6,6*i-5:6*i+6)=mm;

Kmat2=Kmat2+kg;
Mmat2=Mmat2+mg;

end

Kmat2;
Mmat2;

%+++++++%

KG1=zeros(12*el_num+6);MG1=zeros(12*el_num+6);
KG2=zeros(12*el_num+6);MG2=zeros(12*el_num+6);

```

```
KG1(1:6*el_num+6,1:6*el_num+6)=Kmat1;  
MG1(1:6*el_num+6,1:6*el_num+6)=Mmat1;  
KG2(6*el_num+1:12*el_num+6,6*el_num+1:12*el_num+6)=Kmat2;  
MG2(6*el_num+1:12*el_num+6,6*el_num+1:12*el_num+6)=Mmat2;  
  
KMAT=KG1+KG2;  
MMAT=MG1+MG2;  
  
E=eig(inv(MMAT)*KMAT);  
omega=sort(sqrt(E));  
frequency_Hz=omega/(2*pi);  
Hz=frequency_Hz(1)
```

